Published OnlineFirst September 24, 2014; DOI: 10.1158/2159-8290.CD-14-0096

RESEARCH ARTICLE

Access to Follicular Dendritic Cells Is a Pivotal Step in Murine Chronic Lymphocytic Leukemia B-cell Activation and Proliferation

Kristina Heinig[1], Marcel Gätjen[2], Michael Grau[3], Vanessa Stache[1], Ioannis Anagnostopoulos[4], Kerstin Gerlach[2], Raluca A. Niesner[5], Zoltan Cseresnyes[5,6], Anja E. Hauser[5,7], Peter Lenz[3], Thomas Hehlgans[8], Robert Brink[9], Jörg Westermann[10], Bernd Dörken[2,10], Martin Lipp[1], Georg Lenz[10], Armin Rehm[2,10], and Uta E. Höpken[1]

Published OnlineFirst September 24, 2014; DOI: 10.1158/2159-8290.CD-14-0096

ABSTRACT In human chronic lymphocytic leukemia (CLL) pathogenesis, B-cell antigen receptor signaling seems important for leukemia B-cell ontogeny, whereas the microenvironment influences B-cell activation, tumor cell lodging, and provision of antigenic stimuli. Using the murine *Eμ-Tcl1* CLL model, we demonstrate that CXCR5-controlled access to follicular dendritic cells confers proliferative stimuli to leukemia B cells. Intravital imaging revealed a marginal zone B cell–like leukemia cell trafficking route. Murine and human CLL cells reciprocally stimulated resident mesenchymal stromal cells through lymphotoxin-β-receptor activation, resulting in CXCL13 secretion and stromal compartment remodeling. Inhibition of lymphotoxin/lymphotoxin-β-receptor signaling or of CXCR5 signaling retards leukemia progression. Thus, CXCR5 activity links tumor cell homing, shaping a survival niche, and access to localized proliferation stimuli.

SIGNIFICANCE: CLL and other indolent lymphoma are not curable and usually relapse after treatment, a process in which the tumor microenvironment plays a pivotal role. We dissect the consecutive steps of CXCR5-dependent tumor cell lodging and LTβR-dependent stroma–leukemia cell interaction; moreover, we provide therapeutic solutions to interfere with this reciprocal tumor–stroma cross-talk. *Cancer Discov; 4(12); 1448–65. ©2014 AACR.*

See related commentary by López-Guerra et al., p. 1374.

INTRODUCTION

In patients with B-cell chronic lymphocytic leukemia (B-CLL), tumor cell survival and progression are linked to interactions between leukemia cells and nontumor cells in microenvironments of the spleen, peripheral blood, and bone marrow (1–3). Little is known about how CLL cells get access to a putative proliferation and survival niche within lymphoid organs, and a spatial and kinetic resolution of this process is desirable for two reasons. First, the microanatomy of B-cell activation might illuminate the cellular encounters leading to apoptosis resistance versus proliferation induction in CLL cells. Second, signaling events could alter trafficking behavior of leukemia B cells, which is likely relevant for B-cell stimulation.

B-CLL is the most frequent leukemia subtype affecting adults in Western countries (4). It develops as an expansion of clonal mature $CD5^+$ B cells (5, 6), and gene expression profiles of CLL cells show that these malignant B cells resemble antigen-experienced memory B cells (7, 8). The precise cell-of-origin is debated. Depending on differentiation markers, or a putative antigen experience in conjunction with B-cell receptor (BCR) selection, either a marginal zone (MZ) B-2 cell, a B-1 lymphocyte, or a hematopoietic stem cell origin have been proposed (9, 10).

Several genomic aberrations involving karyotypic alterations or mutations in *TP53*, *NOTCH1*, and other markers are frequently reported in CLL cases (3, 11). High T-cell leukemia/lymphoma 1 (*TCL1*) oncogene expression is linked to an aggressive B-CLL phenotype, with leukemic cells displaying a nonmutated immunoglobulin (Ig) receptor and profound *ZAP70* expression (3, 12). A mouse B-CLL model has been developed by introducing a transgene encoding human *Tcl1* under the control of the immunoglobulin heavy chain Eμ-enhancer, resulting in *Tcl1* overexpression at the mostly mature stages of B-cell development (13). *Tcl1* transgenic mice develop B-CLL–like tumors characterized by an expansion of $B220^{lo}IgM^+CD5^+CD11b^+$ cells, initially localized in the peritoneum and, subsequently, in the spleen, bone marrow, and peripheral blood. This B-CLL model has proven suitable to phenocopy several aspects of the human disease, including low proliferative progression, tissue distribution, and B-cell differentiation status.

As in the migration of their normal cellular counterparts, trafficking and homing of CLL cells to and within the tissue microenvironment are regulated by adhesion molecules in concert with the chemokine–chemokine receptor system (14). The homeostatic chemokine receptor CXCR4 has emerged as a key receptor in the recruitment of and cross-talk between malignant B cells and their protective bone marrow microenvironment (15). Expression of secondary lymphoid organ (SLO)–homing receptors, including CCR7 and CXCR5, on human B-cell non-Hodgkin and Hodgkin lymphoma correlates with their dissemination and tissue localization to and within specific SLO compartments (16, 17).

[1]Department of Tumor Genetics and Immunogenetics, Max-Delbrück-Center for Molecular Medicine, MDC, Berlin, Germany. [2]Department of Hematology, Oncology and Tumorimmunology, Max-Delbrück-Center for Molecular Medicine, MDC, Berlin, Germany. [3]Department of Physics, Philipps-University Marburg, Marburg, Germany. [4]Department of Pathology, Charité-Universitätsmedizin Berlin, Campus Mitte, Berlin, Germany. [5]Deutsches Rheumaforschungszentrum, DRFZ, Berlin, Germany. [6]Confocal and 2-Photon Microscopy Core Facility, Max-Delbrück-Center for Molecular Medicine, MDC, Berlin, Germany. [7]Charité-Universitätsmedizin Berlin, Berlin, Germany. [8]Institute for Immunology, University Regensburg, Regensburg, Germany. [9]Garvan Institute of Medical Research, Darlinghurst, New South Wales, Australia. [10]Department of Hematology, Oncology and Tumorimmunology, Charité-Universitätsmedizin Berlin, Campus Virchow-Klinikum, Berlin, Germany.

Note: Supplementary data for this article are available at Cancer Discovery Online (http://cancerdiscovery.aacrjournals.org/).

A. Rehm and U.E. Höpken contributed equally to this article.

Corresponding Authors: Uta E. Höpken, Max-Delbrück-Center for Molecular Medicine, MDC, 13125 Berlin, Germany. Phone: 49-30-94063330; Fax: 49-30-94063390; E-mail: uhoepken@mdc-berlin.de; and Armin Rehm, arehm@mdc-berlin.de

doi: 10.1158/2159-8290.CD-14-0096

Published OnlineFirst September 24, 2014; DOI: 10.1158/2159-8290.CD-14-0096

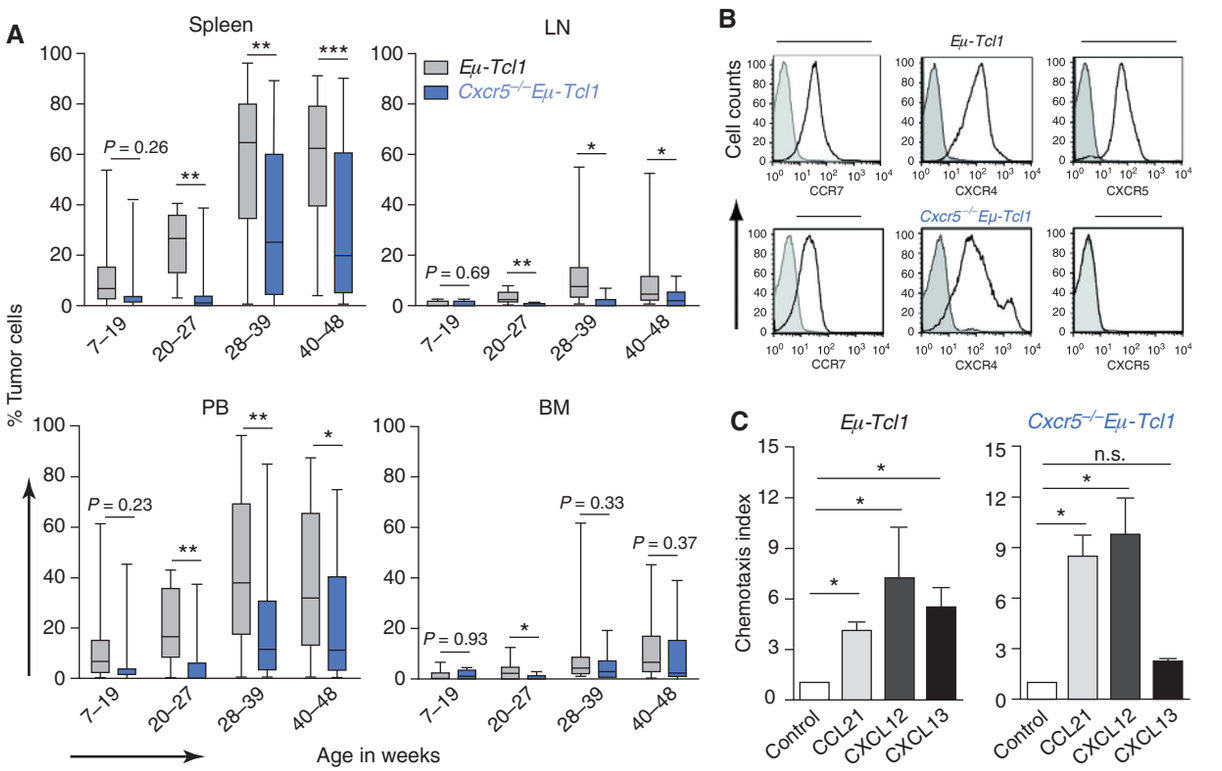

Figure 1. CXCR5 expression accelerates *Eμ-Tcl1* leukemogenesis and is indispensable for tumor cell recruitment to lymphoid B-cell follicles. **A,** tumor load in spleen, lymph node (LN), peripheral blood (PB), and bone marrow (BM) of 7- to 19- ($n = 12$–19), 20- to 27- ($n = 8$–17), 28- to 39- ($n = 36$–52), and 40- to 48- ($n = 12$–52) week-old *Eμ-Tcl1* and 7- to 19- ($n = 9$–15), 20- to 27- ($n = 10$–12), 28- to 39- ($n = 9$–42), and 40- to 48- ($n = 16$–20) week-old *Cxcr5*$^{-/-}$*Eμ-Tcl1* mice. CD19^{+}B220^{low}CD5^{+} tumor cells are presented as percentages of all lymphocytes with means. Error bars indicate Min to Max. *P* values were determined by the unpaired Student *t* test. **B,** chemokine receptor expression on splenic CD19^{+}B220^{low}CD5^{+} gated tumor cells of diseased *Eμ-Tcl1* and *Cxcr5*$^{-/-}$*Eμ-Tcl1* mice ($n = 4$–7 mice/marker; isotype control; shaded curve). **C,** chemotaxis of *Eμ-Tcl1* (left) or *Cxcr5*$^{-/-}$*Eμ-Tcl1* (right) cells toward CCL21 (100 nmol/L), CXCL12 (25 nmol/L), and CXCL13 (300 nmol/L). Error bars indicate mean ± SEM of three independent experiments with triplicates for each chemokine. *P* values were determined by the Mann–Whitney test. (*continued on following page*)

In B-CLL pathogenesis, a predominant role of BCR signaling in CLL ontogeny has emerged (1). Furthermore, it remains still elusive how the microenvironment assumes a central role in B-cell activation and survival. Here, we aimed to link the mechanisms of leukemia cell activation and the microenvironment dependence during CLL pathogenesis in *Eμ-Tcl1* mice. We intravitally visualized the CXCR5-mediated guidance of leukemic B cells toward splenic B-cell follicles via a route normally taken by MZ B cells. In germinal center (GC) light zones, tumor B cells productively interacted with follicular dendritic cells (FDC), which accelerated proliferation and clinical progression. Leukemia cells initiated LTαβ-dependent reciprocal cross-talk with resident follicular stroma cells, leading to CXCL13 release. Selective targeting of stroma-associated CXCL13 and LTβR signaling abrogated this paracrine feedback loop and retarded leukemia growth.

RESULTS

CXCR5-Dependent *Eμ-Tcl1* Tumor Cell Localization within the Growth-Promoting Environment of the Splenic Follicular Compartment

To assess a putative role of CXCR5-governed leukemia cell migration and expansion in a CLL model, we crossed *Eμ-Tcl1* transgenic and *Cxcr5*$^{-/-}$ mice and followed their spontaneous tumor development compared with *Eμ-Tcl1* mice (Fig. 1A). We detected leukemia B cells (CD19^{+}CD5^{+}; Supplementary Fig. S1A–S1C and Fig. 1A) in the spleen and peripheral blood of *Eμ-Tcl1* mice after 2 months. In *Cxcr5*$^{-/-}$*Eμ-Tcl1* mice, disease onset was substantially delayed. At 4 to 6 months of age, tumor cells in *Eμ-Tcl1* mice accounted for 30% to 50% of all lymphocytes, whereas tumor cells were barely detectable in *Cxcr5*$^{-/-}$*Eμ-Tcl1* mice. After >6 months, *Eμ-Tcl1* mice showed a further increased tumor load (>50%) in spleen and peripheral blood, whereas that in *Cxcr5*$^{-/-}$*Eμ-Tcl1* mice was still much lower. At 5 to 6 months of age, we also detected more leukemia B cells in the bone marrow of *Eμ-Tcl1* compared with *Cxcr5*$^{-/-}$*Eμ-Tcl1* mice (Fig. 1A). *Eμ-Tcl1* leukemia cells in the spleen (Fig. 1B) expressed high levels of functional CCR7, CXCR4, and CXCR5 chemokine receptors, as shown *in vitro* by their migration in response to the respective chemokines CCL21, CXCL12, and CXCL13 (Fig. 1C). High expression levels of the homeostatic chemokine receptors were not restricted to the spleen, because lymph node (LN)–, peripheral blood–, and bone marrow–derived leukemia cells also abundantly expressed CCR7, CXCR4, and CXCR5 (Supplementary Fig. S1D). Integrins β1, β2, β7, α4, and αLβ2

Published OnlineFirst September 24, 2014; DOI: 10.1158/2159-8290.CD-14-0096

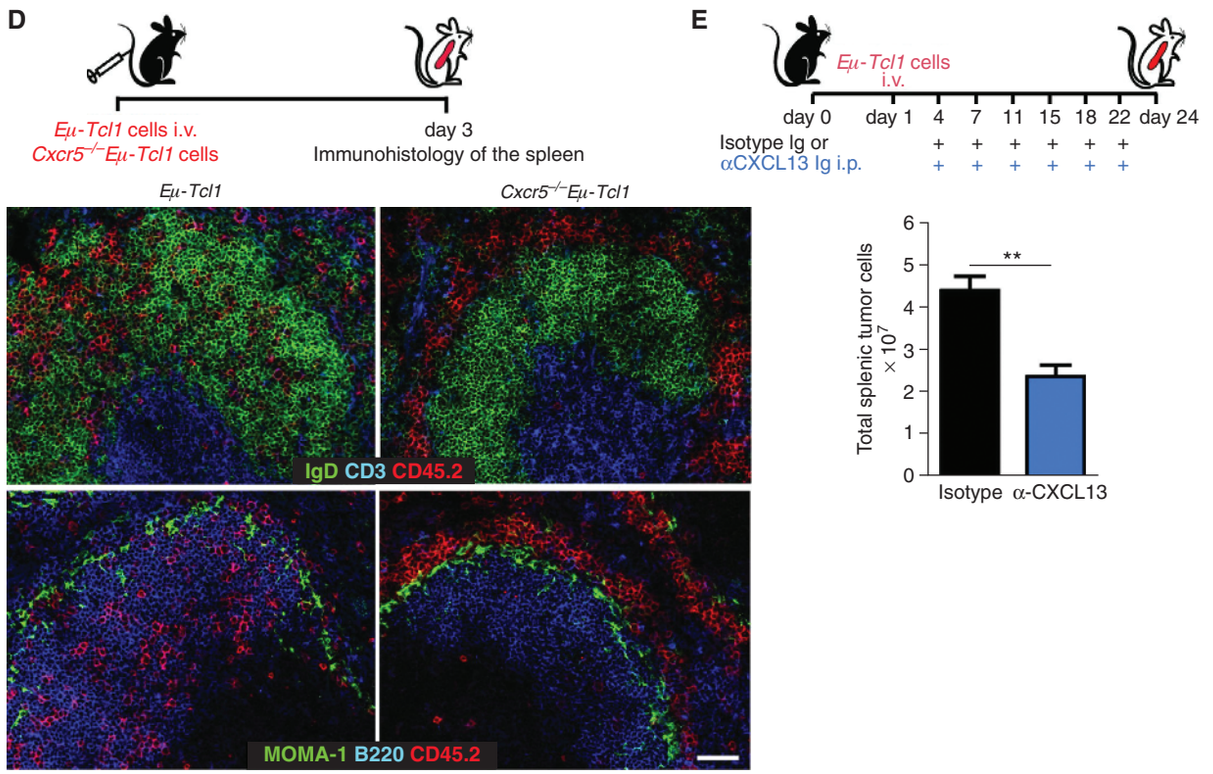

Figure 1. ***(Continued)*** **D,** adoptive transfer of 2×10^7 splenic leukemia cells of *Eμ-Tcl1* and *Cxcr5*$^{-/-}$*Eμ-Tcl1* mice (CD45.2$^+$) into CD45.1$^+$ B6 recipients. Three days after i.v. transfer, spleen sections were stained for CD45.2$^+$ tumor cells, CD3$^+$ T cells, and IgD$^+$ B cells ($n = 8$–9/group; top). Bottom, detection of tumor cells, B cells, and MOMA-1$^+$ metallophilic macrophages ($n = 8$–9/group). Scale bars, 100 μm. **E,** *in vivo* blockage of the CXCL13 signaling pathway by treatment of tumor challenged mice (1×10^6 *Eμ-Tcl1* cells i.v. on day 1) with 50 μg anti-CXCL13 or isotype Ab intraperitoneally (i.p.) at the days indicated ($n = 3$/group). Tumor cell (CD19$^+$B220^{low}CD5$^+$) load was assessed by flow cytometry at day 24. Error bars indicate mean ± SEM. *P* values were determined by the unpaired Student *t* test. *, $P \le 0.05$; **, $P \le 0.01$; ***, $P \le 0.001$. n.s., not significant.

(LFA-1) were readily detected on all *Eμ-Tcl1* leukemia cells, and quantitative real-time PCR (qRT-PCR) revealed substantial expression for LTα, LTβ, and TNFα in *Eμ-Tcl1* and *Cxcr5*$^{-/-}$*Eμ-Tcl1* cells (Supplementary Fig. S2A and S2B). Hence, *Eμ-Tcl1* leukemia B cells are equipped with functional homeostatic chemokine receptors and integrins that enable them for access to SLOs.

We confirmed abundant high CXCR5 expression on human CLL tissue (Supplementary Fig. S2C) and on human peripheral CLL blood samples (Supplementary Fig. S2D). Much weaker expression was observed on CLL cells localized within proliferation centers, which are thought to harbor a proliferative fraction of CLL leukemia B cells (18).

Next, malignant B cells derived from diseased *Eμ-Tcl1* or *Cxcr5*$^{-/-}$*Eμ-Tcl1* mice were adoptively transferred into wild-type (WT) congenic recipients. After 72 hours, leukemia cells were detected in the spleen, peripheral blood, and bone marrow. *Eμ-Tcl1* cells were predominantly localized within splenic B-cell follicles (Fig. 1D). In contrast, *Cxcr5*$^{-/-}$*Eμ-Tcl1* cells were completely absent from B-cell follicles and were mostly found in the MZ outside the metallophilic macrophage ring (MOMA-1$^+$). To further assess whether this follicular localization had any consequences on leukemia progression, we applied a CXCL13 antibody to inhibit CXCR5 signaling. Expansion of adoptively transferred tumor B cells was substantially diminished in spleens of CXCL13-treated mice (Fig. 1E).

Collectively, these data indicate that CXCR5 contributes to accelerated leukemia development, potentially by conferring a survival advantage to *Eμ-Tcl1* tumor cells within the B-cell follicle.

Gene Expression Signatures Indicate a Proliferative Advantage in CXCR5-Expressing *Eμ-Tcl1* Leukemia Compared with *Cxcr5*$^{-/-}$*Eμ-Tcl1* Leukemia

The slower kinetics of tumor growth in *Cxcr5*$^{-/-}$*Eμ-Tcl1* transgenic mice could relate to a reduced proliferation rate. Using genome-wide expression arrays, we examined relative changes in gene expression of splenic leukemia cells derived from diseased *Eμ-Tcl1* versus *Cxcr5*$^{-/-}$*Eμ-Tcl1* mice. Gene set enrichment analysis (GSEA) identified seven different proliferation signatures that discriminated *Cxcr5*$^{+/+}$ from *Cxcr5*$^{-/-}$ leukemias (Fig. 2A and B; Supplementary Fig. S3A). For example, the gene-expression signature of the neighborhood of the cell division cycle 2 (CDC2; G_1–S and G_2–M) in the GNF2 expression compendium (19) predicted a proliferative advantage in CXCR5-expressing *Eμ-Tcl1* tumor cells and included genes involved in cell-cycle regulation, DNA

Published OnlineFirst September 24, 2014; DOI: 10.1158/2159-8290.CD-14-0096

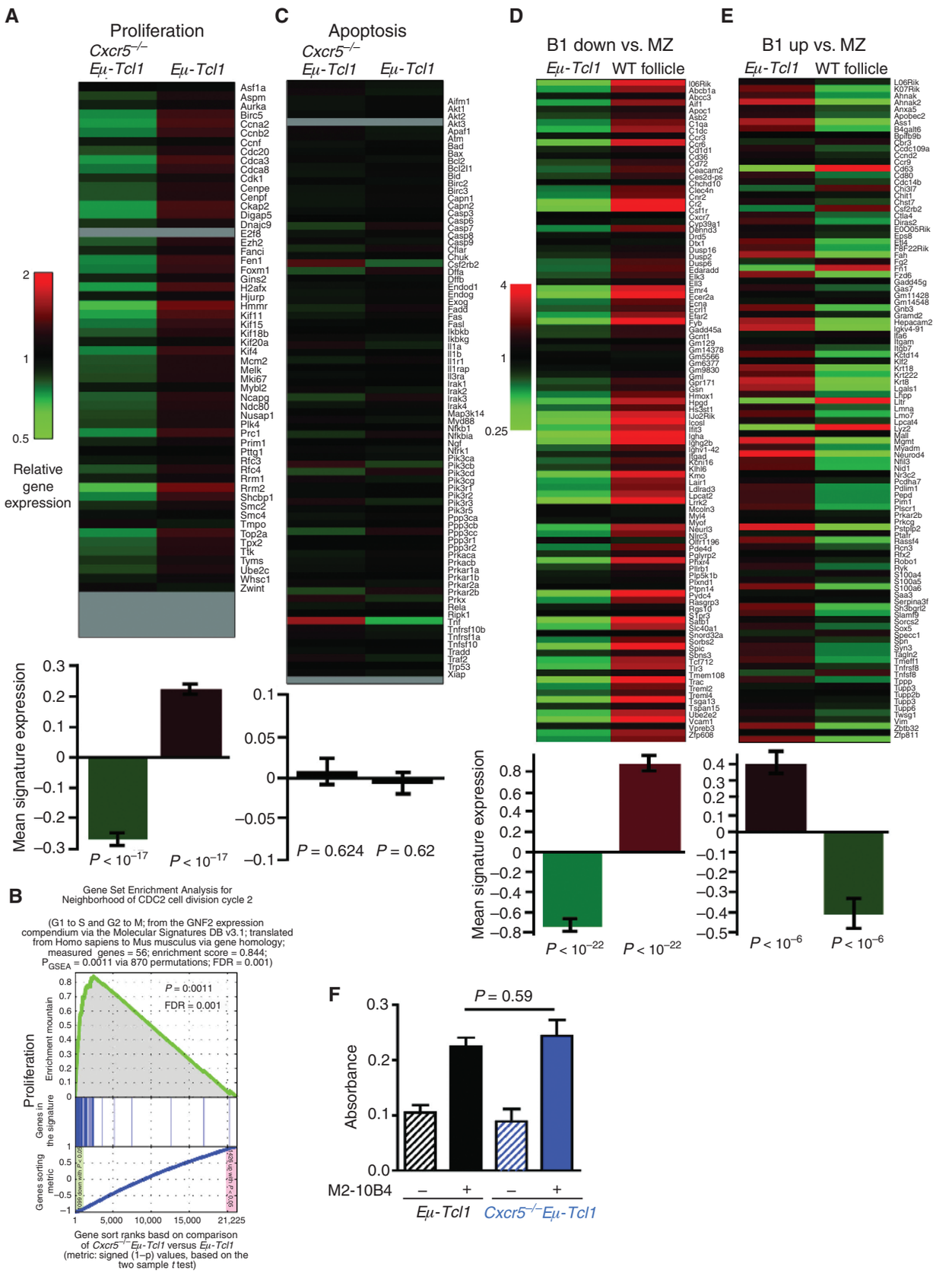

Published OnlineFirst September 24, 2014; DOI: 10.1158/2159-8290.CD-14-0096

synthesis, and protein translation. Conversely, CXCR5$^{-/-}$ versus CXCR5$^{+/+}$ leukemia did not differentially express gene sets of apoptosis-mediating pathways like the Kyoto Encyclopedia of Genes and Genomes (KEGG) apoptosis signature (Fig. 2C; ref. 20).

Eμ-Tcl1 leukemia B cells represent the unmutated and aggressive type of B-CLL (21). A bias toward the restricted use of V_H gene segments was noted, indicating that the expanded CD5$^+$ B-cell population in *Eμ-Tcl1* mice could be derived from B-1 lineage cells. We performed a transcriptome analysis of leukemia cells, murine B-1 B cells, and MZ B cells (Fig. 2D and E). Two gene expression signatures comprised of the top 100 downregulated and upregulated genes in B-1 cells compared with MZ B cells were defined. When gene expression of these signatures was compared in leukemia cells and in follicle cells derived from WT mice, a strikingly higher similarity of *Eμ-Tcl1* leukemia cells to B-1 B cells as compared with MZ B cells was revealed.

Next, we adoptively transferred leukemia cells to synchronize pathogenic events at the onset of the disease (22). Leukemia cells were retrieved and we used qRT-PCR to assess their gene expression pattern, focusing on genes reportedly involved in CLL survival (23). WNT6 and WNT10A were modestly elevated in *Eμ-Tcl1* tumor cells, whereas *Cxcr5*$^{-/-}$*Eμ-Tcl1* leukemia cells showed substantially higher gene expression for the transcription factor RUNX2 (Supplementary Fig. S3B). The cell-cycle inhibitor p21, a transcriptional target of RUNX2 (24), was also upregulated in *Cxcr5*$^{-/-}$*Eμ-Tcl1* leukemia (Supplementary Fig. S3C), indicating that CXCR5 confers *Eμ-Tcl1* tumor cells with a proliferative advantage.

When leukemia cells were cocultured with the FDC/HK cell line, the activities of serine/threonine kinases p42/p44, p38, and AKT were indiscriminable in both genotypes (Supplementary Fig. S3D). In addition, a comparable proliferation rate of WT and CXCR5-deficient tumor cells was detectable when leukemia cells were cocultured with the stroma cell line M2-10B4 (Fig. 2F). This indicates that when tumor cells get access to stromal cell support *in vitro*, their proliferation is supported. *In vivo*, CXCR5 controls this access to a tumor growth-promoting stromal niche.

Eμ-Tcl1 Leukemia Cells Move Directly across the MZ–WP Border to Gain Access to the B-cell Follicle

Lymphocyte transition from the blood into the spleen occurs at the MZ. Follicular B and T cells then migrate along the fibroblastic reticular cell (FRC)–rich MZ bridging channels (MZBC) toward the splenic white pulp (WP) and eventually enter the periarteriolar lymphoid sheaths (PALS). This movement is largely CCR7-dependent (25). In contrast, MZ B cells undergo CXCR5- and S1P1-controlled constitutive shuttling between the MZ and the follicle (26).

It is unknown how CLL cells access the B-cell follicle. Applying a sequential static imaging approach, SNARF-1–labeled tumor or B cells were adoptively transferred into B6 recipients. One to five hours later, spleens were stained with anti-B220 to locate B-cell follicles and anti–MOMA-1 to highlight the border between WP and MZ (Fig. 3A and B). We counted the numbers of labeled *Eμ-Tcl1* leukemia cells or normal B cells in four regions of the spleen: the red pulp (RP; MOMA-1$^-$B220$^-$), MZ (MOMA-1$^+$B220$^+$), B-cell follicle (MOMA-1$^-$B220$^+$), and T/B zone interface (Fig. 3A and B). One hour after transfer, normal B cells were found predominantly in the RP but also in the MZ (Fig. 3B and C), whereas >50% of tumor cells were localized either within the MZ or in B-cell follicles (Fig. 3A and C). Two hours after transfer, B cells were still predominantly located in the RP, with a smaller proportion in the MZ, and single B cells appeared at the T/B–cell border. Tumor cells were equally distributed between MZ and B-cell follicle with a smaller proportion in the RP. Three to five hours after transfer, the proportion of leukemia cells in B-cell follicles further increased, whereas tumor cells remained absent from the T/B–cell border (Fig. 3A–D). In contrast, B lymphocytes transiently accumulated at the T/B zone border (between 2 and 3 hours) before entering the B-cell follicle (3–5 hours; Fig. 3B–D).

The positioning of B cells at the T/B–cell border is regulated by CCR7 and EBI2 chemotactic activity (27). After adoptive transfer, both *Ccr7*$^{-/-}$ and *Ccr7*$^{+/+}$ leukemia cells showed the same direct migratory route from the MZ into B-cell follicles, with an accumulation at the FDCs (Supplementary Fig. S4A). Likewise, *Ebi2*$^{-/-}$*Eμ-Tcl1* cells exhibited the same localization behavior (Supplementary Fig. S4B and S4C). Clinically, spontaneous leukemia development in *Ebi2*$^{-/-}$*Eμ-Tcl1* double-transgenic animals compared with *Eμ-Tcl1* mice revealed no alteration in tumor growth (Supplementary Fig. S4D).

In summary, *Eμ-Tcl1* leukemia B cells directly cross the MZ sinus, reaching the B-cell follicle faster than follicular B cells, and this process is tightly regulated by the CXCL13–CXCR5 signaling axis.

Figure 2. Differential gene expression signatures of *Eμ-Tcl1* and CXCR5-deficient *Eμ-Tcl1* leukemia cells. **A,** gene expression profiling of sorted *Eμ-Tcl1* ($n = 6$) or *Cxcr5*$^{-/-}$*Eμ-Tcl1* ($n = 5$) leukemia cells. Human genes in the signature definition without a homolog mouse gene and genes without measurement data are depicted in gray. Gene expression profiles were analyzed by Gene Set Enrichment Analysis (GSEA). A representative proliferation signature is shown (Molecular Signature DB v3.1; GNF2 CDC2 cancer gene neighborhood). Gene expression levels are shown relative to the mean of all animals and were averaged over all animals of each genotype. The signature average for each genotype is depicted at the bottom (paired Student *t* tests against zero regulation; error bars indicate SEMs). **B,** enrichment plot of the proliferation signature shown in **A**. Blue lines, genes in the signature; the *P* value of the enrichment score (permutation test), and the false discovery rate (relative to the cancer gene neighborhoods subcategory of the Molecular Signature Database v3.1) are indicated. **C,** gene expression profiles of *Eμ-Tcl1*- versus *Cxcr5*$^{-/-}$*Eμ-Tcl1*-derived tumor cells were analyzed by GSEA, as in **A**. In 83 out of 84 gene signatures related to apoptosis a differential regulation between *Eμ-Tcl1* and *Cxcr5*$^{-/-}$*Eμ-Tcl1* animals was not found. Relative expression for all genes belonging to the representative KEGG apoptosis pathway is shown here. The average signature expression determined by the paired Student *t* tests against zero regulation; error bars indicate SEMs. **D** and **E,** B-1 and MZ B cells were compared and the top 100 downregulated (**D**) and upregulated (**E**) genes were identified. Shown are relative gene expression levels of these genes in *Eμ-Tcl1* tumor cells versus WT total follicular cells. Genes found upregulated in B-1 versus MZ B cells were also found upregulated in *Eμ-Tcl1* tumor versus WT total follicular cells and likewise for downregulated genes. **F,** proliferation of *Eμ-Tcl1* or *Cxcr5*$^{-/-}$*Eμ-Tcl1* leukemia cells cocultured with or without a M2-10B4 stromal layer was analyzed by an enzymatic activity assay (CellTiter 96 AQeous One Solution Cell Proliferation Assay from Promega) measuring the absorbance of a formazan product after 48 hours. The quantity of the formazan product as measured by the absorbance at 450 to 540 nm is directly proportional to the number of living cells in the culture. Bars indicate mean ± SEM of three independent experiments; *P* value was determined by the unpaired Student *t* test.

Published OnlineFirst September 24, 2014; DOI: 10.1158/2159-8290.CD-14-0096

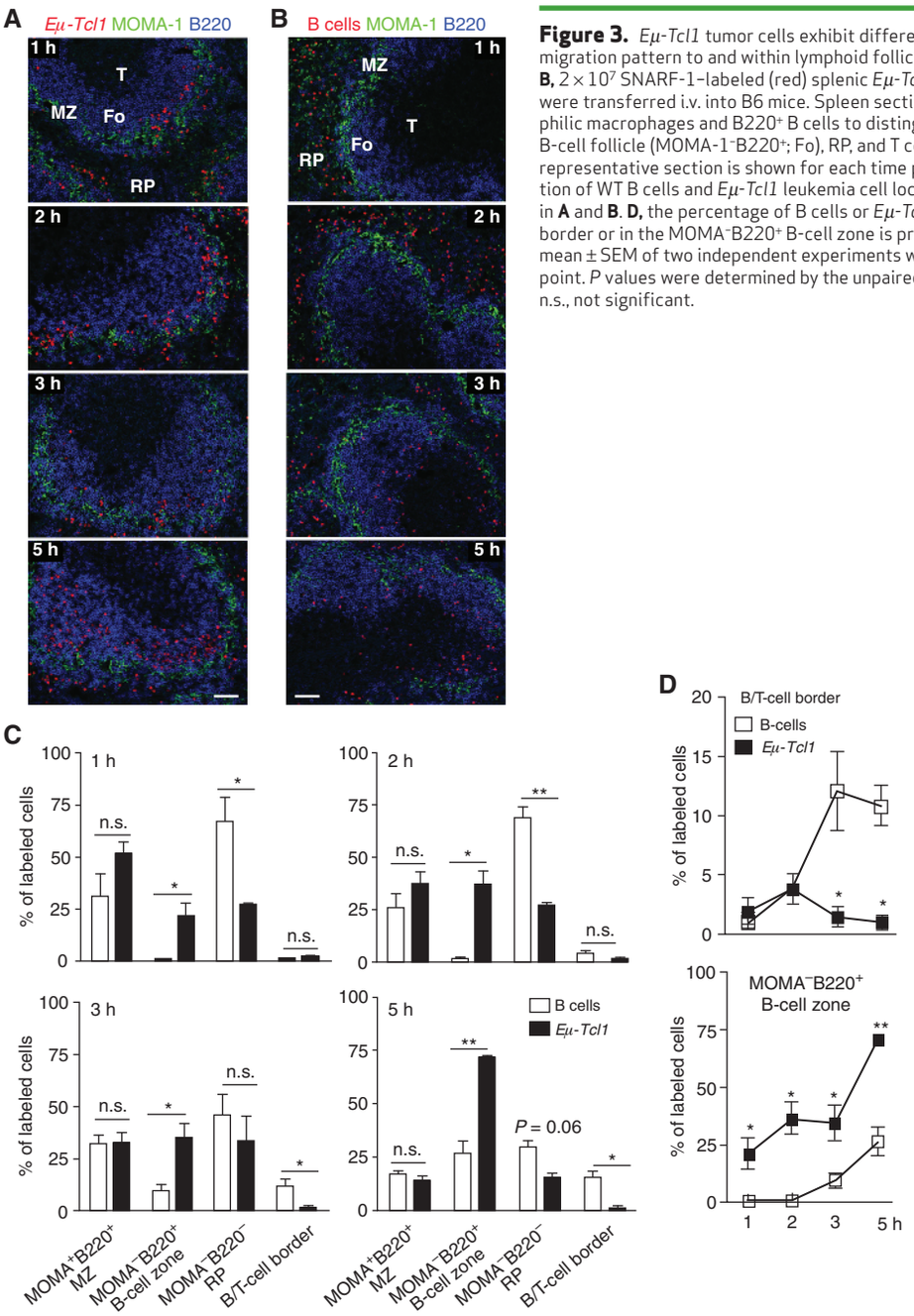

Figure 3. *Eμ-Tcl1* tumor cells exhibit different migratory routes and temporal migration pattern to and within lymphoid follicles compared with B lymphocytes. **A** and **B,** 2×10^7 SNARF-1–labeled (red) splenic *Eμ-Tcl1* leukemia cells or follicular B cells were transferred i.v. into B6 mice. Spleen sections were stained for MOMA-1$^+$ metallophilic macrophages and B220$^+$ B cells to distinguish the MZ (MOMA-1$^+$B220$^+$; MZ), the B-cell follicle (MOMA-1$^-$B220$^+$; Fo), RP, and T cell zone (MOMA-1$^-$B220$^-$; T), and one representative section is shown for each time point. Scale bar, 100 μm. **C,** quantification of WT B cells and *Eμ-Tcl1* leukemia cell localization within the zones as indicated in **A** and **B**. **D,** the percentage of B cells or *Eμ-Tcl1* leukemia cells located at the B/T cell border or in the MOMA$^-$B220$^+$ B-cell zone is presented as a time curve. Bars represent mean ± SEM of two independent experiments with $n = 2$–5 mice for each group and time point. *P* values were determined by the unpaired Student *t* test. *, $P \le 0.05$; **, $P \le 0.01$; n.s., not significant.

Eμ-Tcl1 Leukemia Cells Tightly Colocalize with the Follicular FDC Network and Exhibit Strong ZAP-70/Syk and BTK Activity

FDCs reside within primary follicles and in the GC light zone of secondary B-cell follicles. They express CXCL13, which enables CXCR5-expressing B cells to migrate into lymphoid follicles. Because a strong correlation has been proposed between antigen-stimulated BCR signaling and the clinical course of CLL, we identified follicular stromal networks that locally interact with *Eμ-Tcl1* leukemia cells. Eight hours after transferring leukemia cells, tumor cells tightly intermingled with FDCs (Fig. 4A). These cells stained strongly for the proliferation marker Ki67 (CD45.2$^+$Ki67$^+$), indicating a proliferation-driving interaction. Of all Ki67$^+$ leukemia cells, 77.5% ± 5.8% cells were tightly associated with the FDC networks, whereas only 22.1% ± 3.6% of follicular Ki67$^+$ leukemia cells were located outside of the FDC networks (Fig. 4B).

Next, we simultaneously injected differentially labeled follicular B cells (B220$^+$CD21^{int}CD23^{hi}) with *Eμ-Tcl1* leukemia cells and quantified the proportion of transferred cells within the FDC-rich zone (Fig. 4C). Less than 50% of all transferred follicular B cells were found at the FDC networks. In contrast,

Published OnlineFirst September 24, 2014; DOI: 10.1158/2159-8290.CD-14-0096

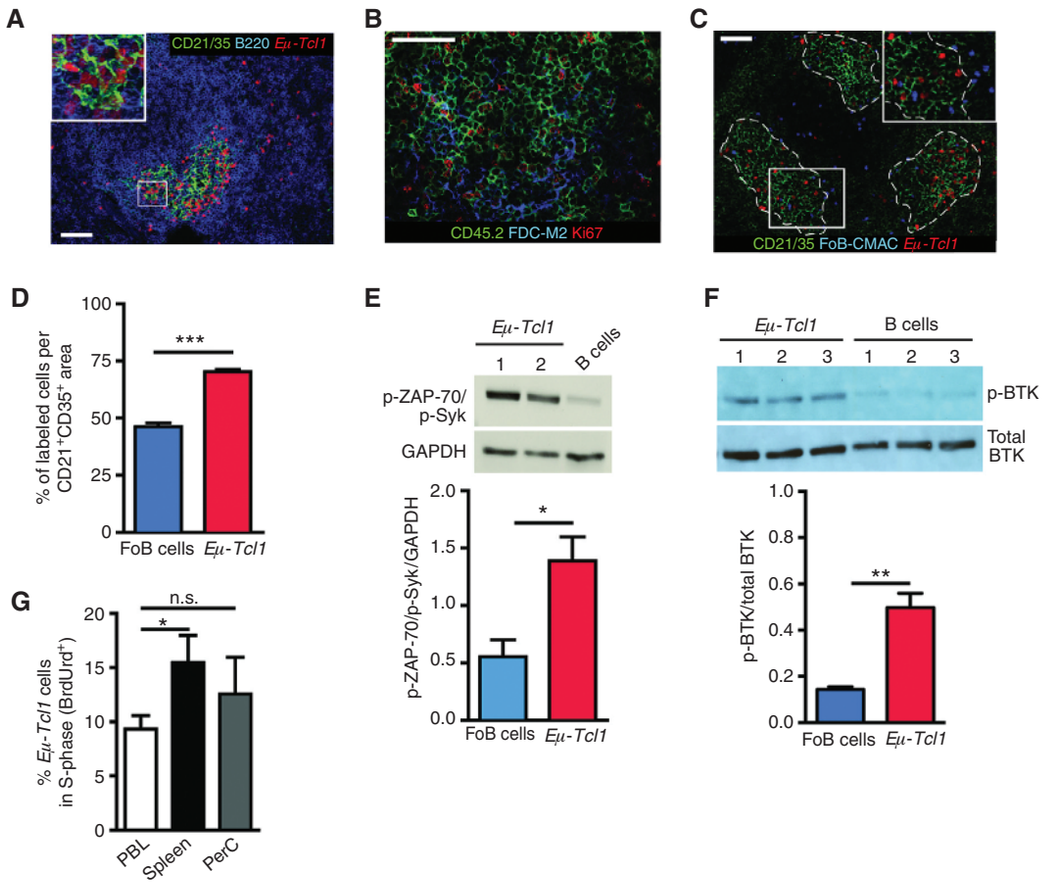

Figure 4. Functional interaction of *Eμ-Tcl1* tumor cells with FDC networks. **A,** splenic *Eμ-Tcl1* leukemia cells were sorted and 2×10^7 SNARF-1–labeled cells (red) were transferred i.v. into recipient mice ($n = 3$). Eight hours later, spleen sections were stained for $CD21^+CD35^+$ FDCs and $B220^+$ B cells. A zoomed inlet (boxed area; left) is additionally shown. Scale bar, 100 μm. **B,** 2×10^7 *Eμ-Tcl1* leukemia cells were transferred i.v. into congenic recipient mice. Three days later, spleen sections were stained for tumor cells ($CD45.2^+$), FDC-$M2^+$ FDCs, and the proliferation marker Ki67 (6–9 sections/mouse; $n = 3$). **C,** splenic follicular B cells ($B220^+CD21^{int}CD23^{hi}$) and *Eμ-Tcl1* lymphoma cells were sorted and labeled with CMAC (FoB, in blue) and SNARF-1 (leukemia cells, in red), respectively. Cells (1×10^7) of both groups were cotransferred into recipient mice ($n = 3$) and localization was analyzed after 8 hours. A representative section and an enlarged inlet of the boxed area are shown. Scale bar, 50 μm. **D,** quantification of the proportion of transferred leukemia cells compared with follicular B cells localized within the FDC rich zone of the B-cell follicle, as marked by the dashed white line in **C**. Error bars indicate mean ± SEM of three independent experiments with a total of nine to 13 analyzed sections. **E,** immunoblot analysis of phosphorylated (p) ZAP-70/Syk from leukemia cells ($n = 14$ mice; #1 and #2 indicate two representative leukemia samples), and follicular B cells ($n = 4$ mice, one representative sample depicted) as a control. Membranes were incubated with anti-phospho-ZAP-70^{Tyr319}/Syk^{Tyr352} (top), and anti-GAPDH (bottom). Bar diagram depicts the quantification of the ratios. Error bars indicate mean ± SEM. **F,** immunoblot analysis of phosphorylated and total BTK from leukemia cells ($n = 3$ mice; #1–3 indicate three leukemia samples), and follicular B cells ($n = 3$ mice, #1–3; three samples) as a control. Membranes were incubated with anti-p-BTK (top), and total BTK (bottom). Bar diagram depicts the quantification of the ratios. Error bars indicate mean ± SEM. **G,** *Eμ-Tcl1* mice with a tumor burden of 21% to 25% ($n = 10$) in peripheral blood were injected i.p. with 1 mg BrdUrd for 3 days. Peripheral blood (PBL), spleen, and peritoneal cavity (PerC)-derived *Eμ-Tcl1* leukemia cells were analyzed for BrdUrd uptake. (*continued on next page*)

more than 70% of leukemia cells strongly colocalized with FDCs (Fig. 4D).

Consistent with the animal model, FDCs could be detected in human CLL specimens at variable rates and shapes, ranging from distinct reticular forms to more complex networks (Supplementary Fig. S5).

Leukemic cells of patients with progressive CLL express the protein tyrosine kinase ZAP-70, which is functionally associated with increased BCR signaling (28). Another tyrosine kinase that is uniformly overexpressed and constitutively active in CLL is Bruton's tyrosine kinase (BTK; refs. 29–31). Here, using an antibody that cross-reacts with phosphorylated (p) ZAP-70 and p-Syk (32), we showed substantially enhanced expression of p-ZAP-70/Syk in *Eμ-Tcl1* leukemia cells compared with B lymphocytes. This finding was corroborated with a p-BTK antibody (Fig. 4E and F), indicating that *Eμ-Tcl1* leukemia cells exhibit increased BCR activity.

BCR engagement and growth factor supply could depend on the environmental context. Here, tissue-resident leukemia cells from the spleen showed an enhanced proportion of cells in S-phase ($BrdUrd^+$), suggesting a stronger stimulus in SLOs compared with cells derived from peripheral blood (Fig. 4G). Thus, *Eμ-Tcl1* leukemia cell contacts to FDC networks could be a prerequisite for tumor cell proliferation that is enhanced by BCR signaling and local cytokine provision.

Published OnlineFirst September 24, 2014; DOI: 10.1158/2159-8290.CD-14-0096

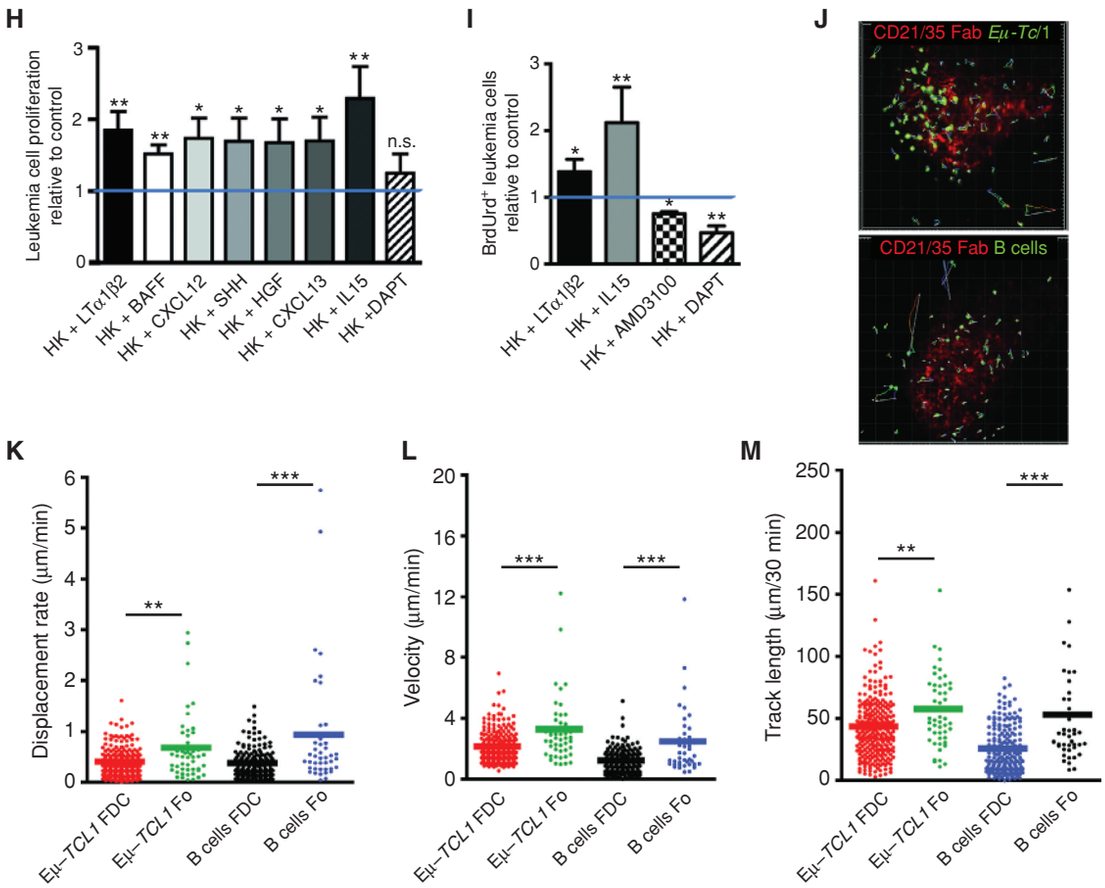

Figure 4. ***(Continued)*** **H** and **I,** splenic-derived *Eμ-Tcl1* leukemia cells (1×10^5) were seeded in triplicate on top of unstimulated (control group) or LTα1β2-prestimulated FDC/HK stroma cells alone, or together with cytokines, growth factors, the CXCR4 antagonist AMD3100 or the Notch inhibitor DAPT, as indicated. After 72 hours, viable leukemia cells were counted (**H**). In **I,** after 24 and 48 hours, cultures were supplemented with 10 μmol/L BrdUrd and BrdUrd uptake was analyzed by flow cytometry 72 hours thereafter. Results are shown as *x*-fold cell proliferation relative to control (FDC/HK + *Eμ-Tcl1* leukemia B cells), set arbitrarily to 1 [indicated by a horizontal line; $n = 7$ (**H**), separate *Eμ-Tcl1* cell clones tested]. Error bars indicate mean ± SEM of five to seven independent experiments. *P* values were determined by the Mann–Whitney test. Tracks of motile *Eμ-Tcl1* leukemia cells (**J**; top) or motile B lymphocytes (**J**; bottom) that are localized within the B-cell follicle at the FDCs, visualized by staining with AF568-labeled anti-CD21$^+$CD35$^+$ Fab fragments (red), are projected onto an image of the entire *z* stack representing a midpoint in the imaging time period of a representative experiment from two independent experiments ($n = 4$ mice/group). Quantitation of displacement rate (**K**), track velocity (**L**), and track length of follicle (Fo)- or FDC-located B cells and *Eμ-Tcl1* lymphoma cells (**M**). Means and significance calculated by the unpaired Student *t* test are shown. *, $P \le 0.05$; **, $P \le 0.01$; ***, $P \le 0.001$; n.s., not significant.

To further dissect these mechanisms, we cocultured seven different *Eμ-Tcl1* leukemia cell clones in the presence of FDC/HK cells (33). When HK cells were prestimulated with LTα1β2, an almost 2-fold higher survival rate of leukemia cells as compared with HK cells alone was seen. This indicated that engagement of the LTβR could induce provision of B-cell growth factors (Fig. 4H). Next, we mimicked cytokine and growth factor conditions that were suggested to support either GC B-cell proliferation or follicular B-cell lymphoma expansion (34, 35). When supplemented, a substantial increase in cell proliferation was obtained for BAFF, CXCL12, Sonic hedgehog (SHH), hepatocyte growth factor (HGF), CXCL13, and IL15 (Fig. 4H). The use of the γ-secretase inhibitor DAPT, and thus NOTCH pathway blockade, served as a negative control. To discriminate between an antiapoptotic effect and a proliferation induction, we repeated this assay for selected cytokines and measured instead BrdUrd uptake. We observed enhanced proliferation rates of *Eμ-Tcl1* leukemia cells (BrdUrd$^+$) after stimulation with LTα1β2 and an even stronger proliferation in the presence of IL15 (Fig. 4I). Treatment of cocultures with the CXCR4 antagonist AMD3100 inhibited BrdUrd uptake (Fig. 4I), which supports the notion that the CXCR4 signaling directly stimulates proliferation of CLL cells. Inclusion of the Gαi/o-protein inhibitor pertussis toxin (PTX) considerably diminished leukemia B-cell viability in HK cocultures (Supplementary Fig. S6A). Hence, BrdUrd uptake could not be reliably determined because of the predominant fraction of apoptotic leukemia cells.

In accordance, when human CLL cells were cocultured with FDC/HK cells, enhanced proliferation of CLL cells was also observed and could be further enhanced by adding IL15 (Supplementary Fig. S6B). Prestimulation with LTα1β2 had a modest effect, which might be explained by higher endogenous expression of LTα and LTβ in human CLL cells (Fig. 7E).

Published OnlineFirst September 24, 2014; DOI: 10.1158/2159-8290.CD-14-0096

If antigen recognition is important for *Eμ-Tcl1* leukemia cell growth, then restricting the antigen specificity of leukemia cells against an irrelevant antigen might reduce their fitness *in vivo*. We generated *Eμ-Tcl1* × BCR^{HEL} double-transgenic mice and analyzed them after repetitive immunization with the cognate antigen HEL or without (Supplementary Tables S1 and S2) for the development of a clonal B-CLL–like disease. Leukemia cell development equipped with the cognate BCR^{HEL} could not be observed in nonimmunized or HEL-immunized mice, indicating that sole stimulation of the BCR^{HEL} does not confer sufficient signaling to promote *Eμ-Tcl1* leukemia development.

The Dynamics of *Eμ-Tcl1* Leukemia Cell Localization in the $CD21^+CD35^+$ GC Light Zone

The localization of *Eμ-Tcl1* tumor cells near FDCs suggested that this network might provide the combined chemoattractant, nutritive, and antigenic stimuli for BCR engagement. To visualize the dynamic behavior of *Eμ-Tcl1* leukemia cells in relation to FDCs, we injected Alexa Fluor 568–conjugated anti-CD21/CD35 Fab fragments for intravital FDC staining (Supplementary Fig. S7), together with CFDA-labeled *Eμ-Tcl1* leukemia or B cells. During a 30-minute imaging period, we tracked individual motile *Eμ-Tcl1* leukemia cells or B cells that were localized within the B-cell follicle or close to the FDCs for as long as the cells remained within the z stacks (height, 40–50 μm) of optical sections (Supplementary Movies S1 and S2). Tracks of motile leukemia or B cells were also projected onto an image of the entire z stack, representing a midpoint in the imaging time period (Fig. 4J). We could distinguish between a more stationary FDC-associated and a more motile follicular-located leukemia cell population based on total displacement from their origin (Fig. 4K), track velocity (Fig. 4L), and total track length (Fig. 4M).

All three parameters were substantially decreased when leukemia cells were close to the FDC networks, as opposed to those located within the outer B-cell follicle (Fig. 4K–M; Fig. 4J, top; Supplementary Movie S1). This association was also obtained in follicular B cells (Fig. 4K–M and Supplementary Movie S2), but fewer B cells were associated with FDCs (Fig. 4D and J, bottom). We conclude that the decreased displacement rate and increased interaction time of leukemia B cells with FDCs could result from the tumor cells' cognate nature and their ability to encounter antigen-laden FDCs.

To assess follicular *Eμ-Tcl1* leukemia positioning following the organization of GCs into dark and light zones, we immunized B6 mice with sheep red blood cells. GC B-cell positioning in the dark zone is crucially dependent on high CXCR4 expression (36). SNARF-1–labeled tumor cells were i.v. transferred; 8 hours later, splenic sections were stained for PNA^+ GCs (centroblasts; dark zone), $CD21^+CD35^+$ FDC networks (light zone), and IgD^+ B-cell follicles (Fig. 5A). Tumor cells were also pretreated with the CXCR4 antagonist AMD3100 (Fig. 5B–D). *Eμ-Tcl1* leukemia cells localized exclusively in the $CD21^+CD35^+$ GC light zone, independently of CXCR4-signaling inhibition (Fig. 5B). Inhibition of CXCR4 signaling after AMD3100 treatment was confirmed *in vitro* in a chemotaxis assay (Fig. 5D).

The sphingosine-1-phosphate receptor S1PR2 helps to confine B cells to the GC (37). GC B cells showed the highest gene expression of *S1pr2*. In contrast, *Eμ-Tcl1* leukemia cells exhibited low *S1pr2* expression comparable to the amounts of *S1pr2* in MZ B cells (Fig. 5E). Collectively, *Eμ-Tcl1* leukemia cells are predominantly recruited to the $CD21^+CD35^+$ GC light zone, but they do not access the PNA^+ dark zone.

In Irradiated Mice *Eμ-Tcl1* Leukemia Cells Exhibit Enhanced Proliferation in Close Proximity to FDCs

Clinically, an unresolved problem in the treatment of indolent lymphoma is its propensitiy to relapse and to progressively develop chemoresistance. The close association of *Eμ-Tcl1* leukemia cells with FDCs raised the question of whether tumor cells might reciprocally support or initiate stromal cell network differentiation. To analyze the mechanisms of a putatively stroma-regulated treatment failure, we first assessed the stroma-inducing capacity of tumor cells in *Rag2*$^{-/-}$ mice that are devoid of mature lymphocytes and lack FRCs and FDCs. These mice still have $MAdCAM\text{-}1^+$ marginal reticular cells (MRC), which produce CXCL13 and express the LTβR. Over a 21-day observation period, *Eμ-Tcl1* leukemia cells induced formation of follicular-like CXCL13-expressing FDC ($CD21^+CD35^+$) networks in *Rag2*$^{-/-}$ mice (Supplementary Fig. S8A). Leukemia-loaded spleen also upregulated CXCL13 und LTβ gene expression (Supplementary Fig. S8B).

Radiotherapy eliminates hematopoietic cells, whereas mesenchymal stromal elements survive. To assess whether residual leukemia cells could exploit stromal contacts and engage with FDCs and MRCs, we transferred *Eμ-Tcl1* cells into irradiated congenic recipients. Although essentially all benign $B220^+$ B cells were depleted after 48 hours, FDCs persisted and the MRC ring expanded (Fig. 6A, top left). Transferred CLL cells accumulated around the FDC networks in an even stronger manner than in untreated mice (Fig. 6A, bottom). Functionally, transfer into irradiated hosts conferred tumor cells with an enhanced proliferative capacity (Fig. 6B and C), and the rate of tumor cells in close proximity to FDC networks that stained strongly for Ki67 was substantially higher compared with untreated controls (Fig. 6B). Irradiation of mice substantially enhanced splenic *Baff* gene expression about 4-fold, whereas APRIL was weaker upregulated (Fig. 6D). We confirmed expression of the corresponding cytokine receptor BAFFR on leukemia cells (Fig. 6E).

To demonstrate that irradiation enhances proliferation in a BAFF-dependent manner, we transferred tumor cells together with a blocking anti-BAFF antibody into irradiated mice. Treatment with the anti-BAFF antibody completely abrogated irradiation-induced proliferation in *Eμ-Tcl1* tumor cells (Fig. 6F).

Taken together, CLL cells are recruited to mesenchymal stromal cells, which in turn promote chemokine-mediated tumor cell attraction, growth acceleration through BCR stimulation, and paracrine provision of cytokines.

Stromal LTβR Signaling Is Crucial for Maintaining FDC Structures and Accelerates *Eμ-Tcl1* Leukemia Progression

FDC stimulation with cell-bound LTαβ or soluble LTα/TNFR1 agonist can induce the expression of CXCL13 and other cytokines (38). Because the leukemia cell itself was also a source of lymphotoxin (Supplementary Fig. S2B), we

Published OnlineFirst September 24, 2014; DOI: 10.1158/2159-8290.CD-14-0096

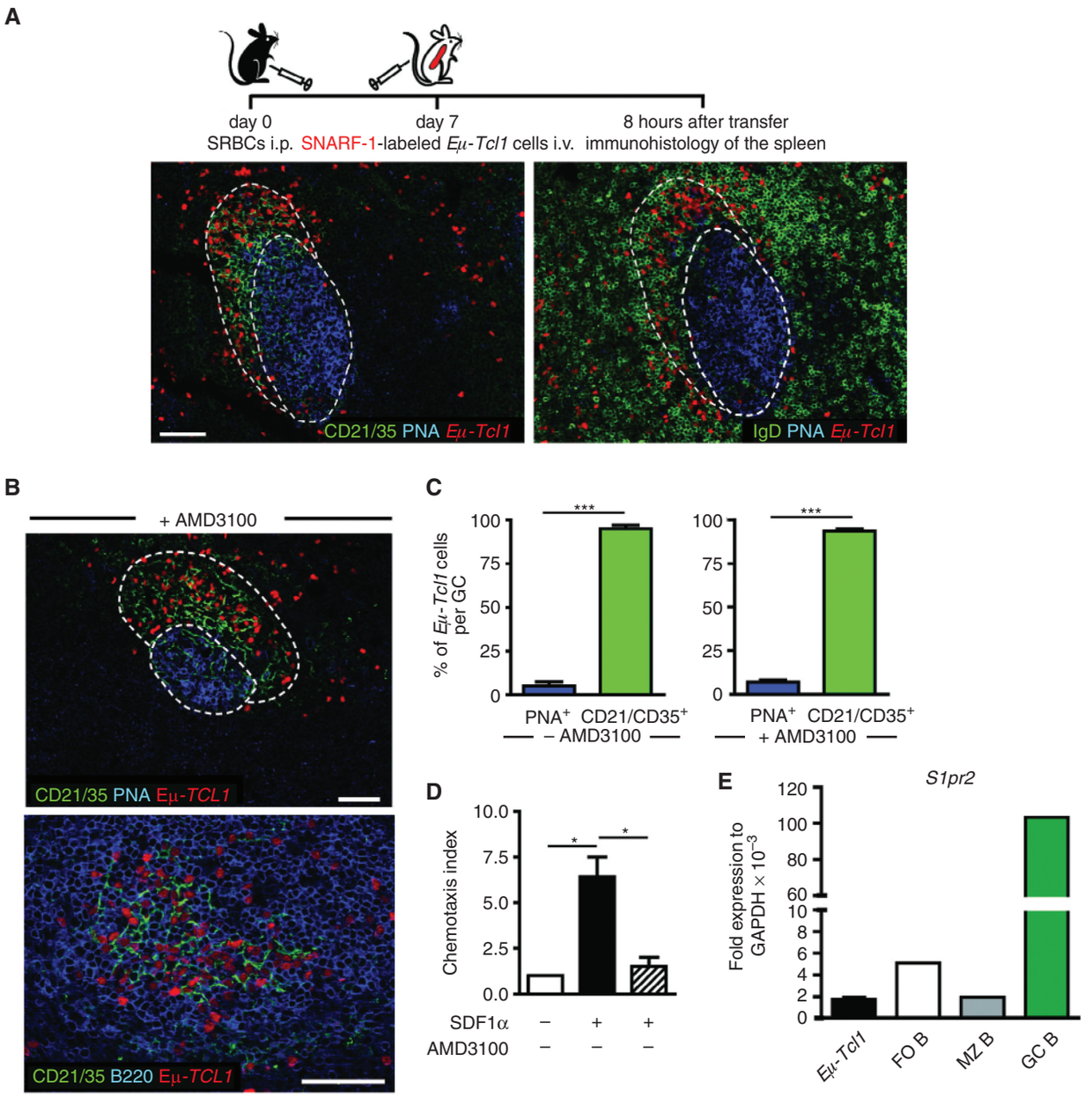

Figure 5. *Eμ-Tcl1* tumor cells localize in the GC-associated FDC-rich light zone independently of *Cxcr4* and *S1pr2* signaling. **A,** WT mice were immunized with sheep red blood cells (SRBC). At day 7, 2×10^7 SNARF-1–labeled sorted splenic *Eμ-Tcl1* tumor cells were transferred i.v. into recipients. Eight hours later, localization of tumor cells (red) was detected in splenic sections by staining for GC-associated FDC-rich light zone ($CD21^+CD35^+$) and PNA^+ dark zone (left) or by staining of IgD^+ B-cell follicular areas and PNA^+ dark zone (right). Two consecutive slides were stained. Scale bar, 50 μm. **B,** B6 mice were immunized as in **A**. At day 8, 2×10^7 sorted splenic *Eμ-Tcl1* leukemia cells were pretreated without AMD3100 (two independent experiments) or with AMD3100 (three independent experiments), followed by i.v. transfer into recipient mice. Eight hours later, localization of tumor cells (red) was detected in splenic sections by staining for GC-associated FDC-rich light zone ($CD21^+CD35^+$) and PNA^+ dark zone (top) and for $CD21^+CD35^+$ FDCs and $B220^+$ B cells (bottom). **C,** quantification of the proportion of leukemia cells within the light zone (green) or within the PNA^+ dark zone (blue). Bars represent mean ± SEM of three to five independent experiments. **D,** chemotaxis of *Eμ-Tcl1* tumor cells toward CXCL12 with and without treatment with AMD3100. Bars represent mean ± SEM of two to four independent experiments with triplicates per each group. *P* values were determined by the Mann–Whitney test. *, $P \le 0.05$; ***, $P \le 0.001$. **E,** qRT-PCR of *S1pr2* in sorted tumor cells of *Eμ-Tcl1* ($n = 4$) mice, and in follicular B ($B220^+CD21^{lo}CD23^{hi}$; Fo B), MZ B ($B220^+CD21^{hi}CD23^{lo}$; MZ B), and GC B ($B220^+GL7^+Fas^+$; GC B) cells (one experiment with 3 mice/group). Transcript expression was normalized to *Gapdh*. Error bars indicate mean ± SEM.

Published OnlineFirst September 24, 2014; DOI: 10.1158/2159-8290.CD-14-0096

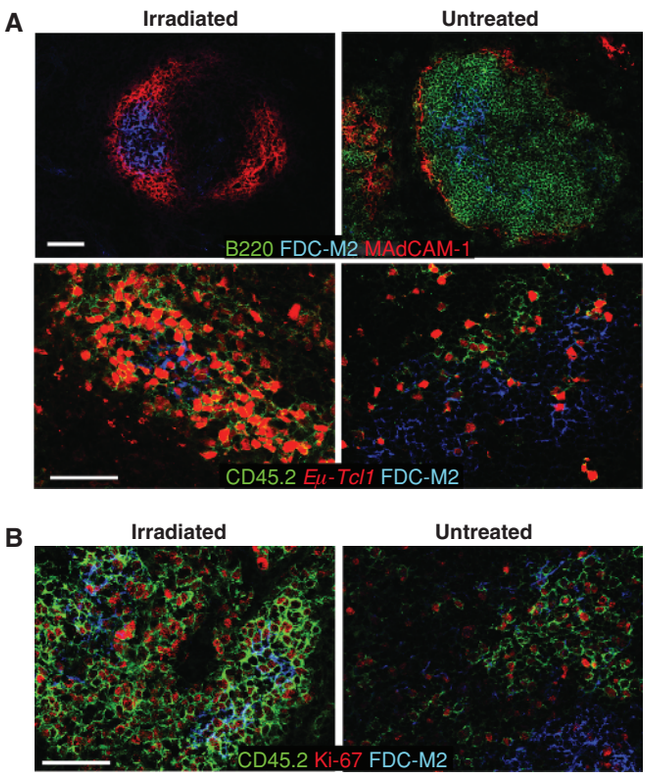

Figure 6. *Eμ-Tcl1* tumor cells localize at radio-resistant FDC networks and exhibit stronger proliferation in the spleens of irradiated mice. **A,** spleens of lethally irradiated (9.25 Gy) or untreated B6 CD45.1 mice were harvested 48 hours ($n = 2$/group) after treatment and stained for $B220^+$ B cells, MAdCAM-1^+ MRCs, and FDC-$M2^+$ stromal cell networks. Representative sections are shown (top). SNARF-1-labeled *Eμ-Tcl1* cells (2×10^7; CD45.2) were adoptively transferred into lethally irradiated recipients ($n = 3$) or into nonirradiated controls ($n = 2$). Forty-eight hours after tumor challenge, spleen sections were stained with CD45.2^+ and FDC-$M2^+$ (blue; bottom) or **B,** CD45.2^+, FDC-$M2^+$, and Ki67^+ antibodies. Representative sections are shown. Scale bars, 100 μm. **C,** eFluor670-labeled *Eμ-Tcl1* leukemia cells ($2–5 \times 10^6$) were adoptively transferred into irradiated mice ($n = 3$) or into untreated recipients ($n = 2$). Forty-eight hours later, proliferation of splenic tumor cells was evaluated according to eFluor670 dilution; a representative histogram shows staining of tumor cells recovered from untreated or irradiated mice. **D,** splenic *Baff* and *April* mRNA transcripts of irradiated or nonirradiated mice with or without tumor cell challenge ($n = 2–3$ mice/group). Transcript expression was normalized to *Gapdh*. Error bars indicate mean ± SEM. **E,** surface expression of BAFFR on splenic *Eμ-Tcl1* leukemia cells ($CD19^+CD5^+$; $n = 5$ transgenic *Eμ-Tcl1* mice) was confirmed by flow cytometry (isotype Ig control, shaded curve; anti-BAFFR Ig, solid line). **F,** blockage of the BAFF signaling pathway by injecting 50 μg anti-BAFF or isotype Ab together with $5–10 \times 10^6$ eFluor670-labeled *Eμ-Tcl1* leukemia cells i.v. ($n = 3–4$/group). Forty-eight hours later, proliferation of splenic tumor cells was evaluated according to eFluor670 dilution; a representative histogram shows staining of tumor cells recovered from isotype or anti-BAFF-treated irradiated mice (left). Relative proportion of proliferated leukemia cells from isotype and anti-BAFF-treated irradiated mice compared with cells from nonirradiated mice (set arbitrarily to 100%; $n = 3$ independent experiments) are depicted as bars ± SEM (right). Means and significance calculated by the unpaired Student *t* test are shown. *, $P \leq 0.05$; **, $P \leq 0.01$.

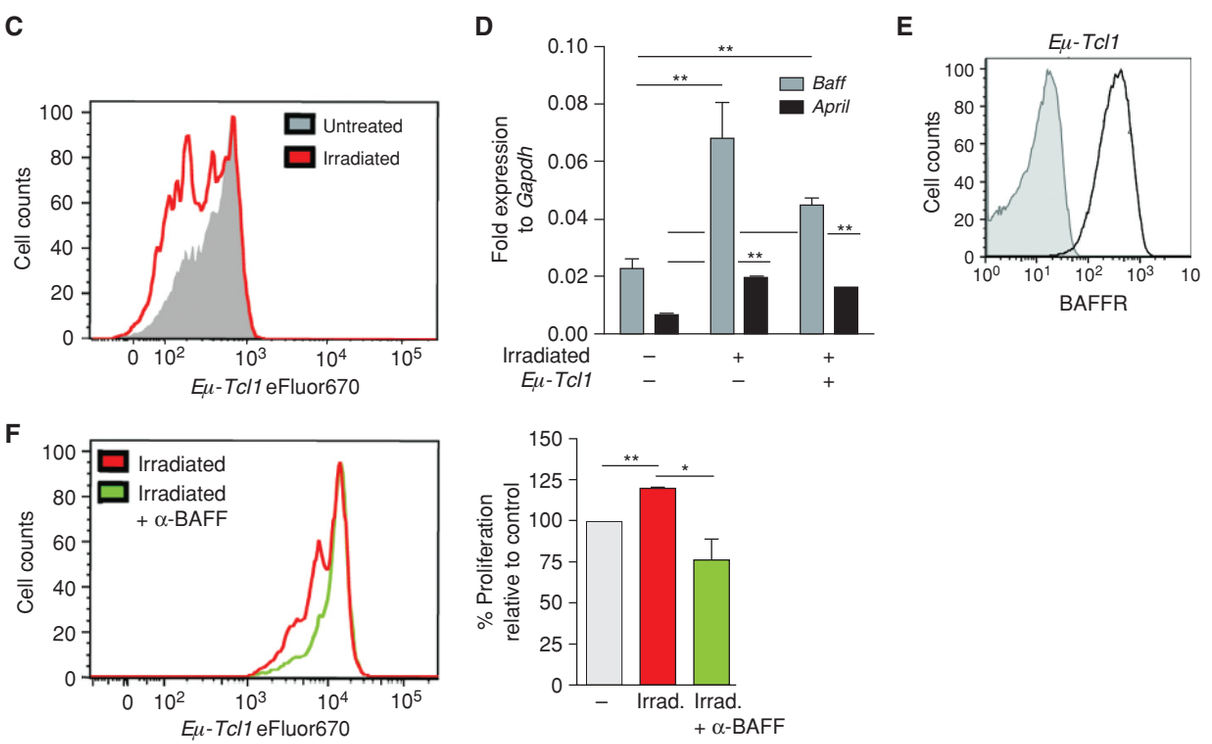

Published OnlineFirst September 24, 2014; DOI: 10.1158/2159-8290.CD-14-0096

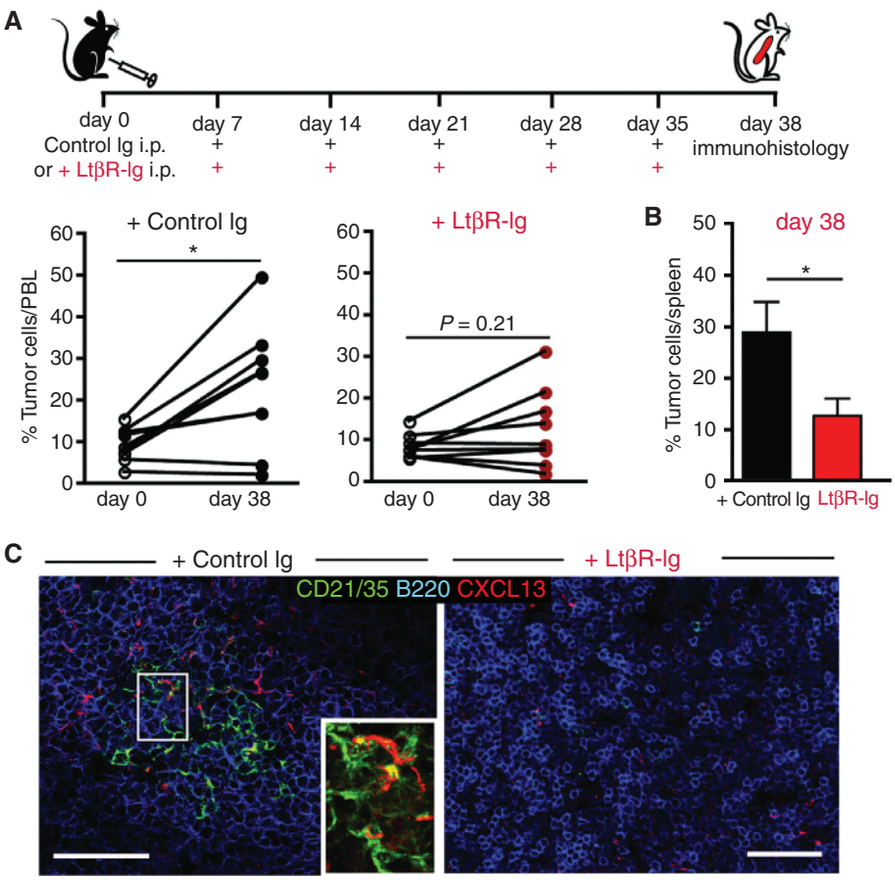

Figure 7. Stromal LTα–LTβR signaling is crucial for maintaining FDC structures and drives *Eμ-Tcl1* leukemia progression. **A** and **B,** *in vivo* blockage of the LTβR signaling pathway by treatment of *Eμ-Tcl1* mice with 100 μg LTβR-Ig ($n = 9$; right) i.p. in 7-day intervals starting on day −1 up to day 35 or control mouse IgG1 (MOCP21; $n = 9$; left). Tumor load was assessed at day 0 and 38 in peripheral blood (PBL; **A**), and at day 38 in (**B**) spleens. Error bars indicate mean ± SEM. *P* values in **A** were determined by the Wilcoxon signed rank test; in **B**, the Mann–Whitney test was applied. **C,** spleen sections (day 38) were stained for $B220^+$ B cells, $CD21^+CD35^+$ FDC networks, and CXCL13 expression. A representative section of each group is shown. Scale bar, 50 μm. (*continued on following page*)

hypothesized that leukemia cell–associated LTαβ conferred the ligand for LTβR activation on FDCs and MRCs. To assess this regulatory feedback loop, we inhibited LTαβ–LTβR signaling in *Eμ-Tcl1* mice using an LTβR–Ig fusion protein. Spontaneously diseased *Eμ-Tcl1* mice with a 5% to 15% tumor load in peripheral blood were treated with the decoy receptor protein LTβR–Ig. *Eμ-Tcl1* mice treated with a control Ig showed a substantially increased tumor load in peripheral blood from days 0 to 38 of treatment, whereas no such increment was observed in LTβR–Ig–treated mice (Fig. 7A). Tumor load in the spleen of isotype-treated *Eμ-Tcl1* mice was also higher than in LTβR–Ig-treated animals (Fig. 7B). Immunohistology showed substantial FDC disappearance (Fig. 7C) and a severe disturbance of MAdCAM-1^+ and BP-3^+ B-cell follicle stromal structures (Supplementary Fig. S9A) in LTβR–Ig–treated animals. Splenic *Ccl21* and *Cxcl13* gene expressions were lower in LTβR–Ig–treated *Eμ-Tcl1* mice compared with controls (Fig. 7D).

Supporting a pathogenic role of LTβR signaling, disease onset and progression were substantially delayed in *Lt*$\alpha^{-/-}$*Eμ-Tcl1* double-transgenic mice compared with *Eμ-Tcl1* animals (Supplementary Fig. S9B). Hence, tumor cell production of LTα accelerates tumor growth. Conversely, interference with LTβR signaling leads to growth reduction in a murine CLL model.

In line with the data from *Eμ-Tcl1* mice, lymphotoxin and TNFα transcripts could be detected in sorted human CLL cells, normal B cells, and in the human B-CLL line MEC-1 (Fig. 7E). Adoptive transfer of MEC-1 cells into *NOD/SCID/c-γ-chain*$^{-/-}$ mice elicited a follicular-like FDC network (Fig. 7F, left), a process which could be completely abrogated by LTβR–Ig treatment (Fig. 7F, right). Thus, LTβR signaling is an essential part of the reciprocal relationship between leukemia B cells and mesenchymal stromal cells.

DISCUSSION

In this study, we tracked the trafficking routes of murine CLL cells into protective microenvironmental niches in SLOs, and identified FDCs as a crucial resident stromal cell population that supports consecutive steps of leukemia pathogenesis. Using the *Eμ-Tcl1* transgenic mouse (13) as a CLL model, we also obtained functional evidence that the chemokine

Published OnlineFirst September 24, 2014; DOI: 10.1158/2159-8290.CD-14-0096

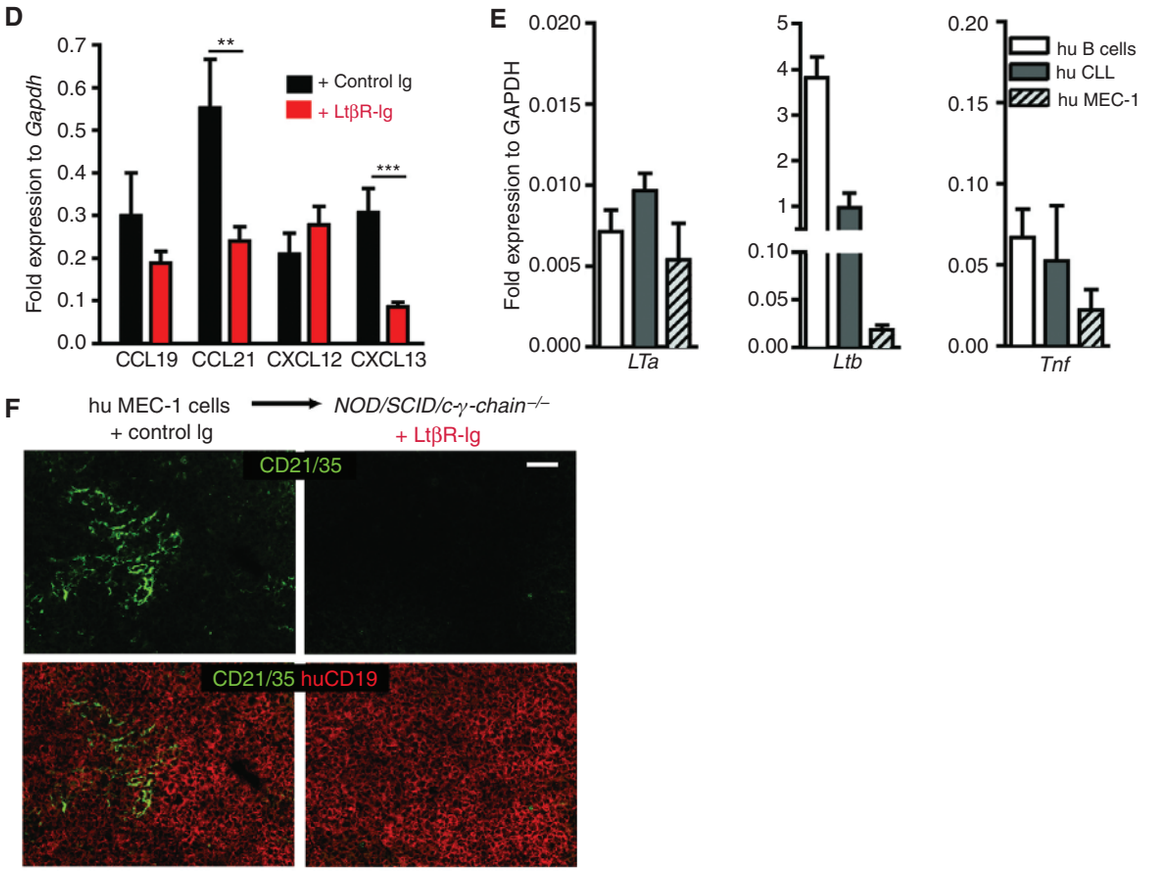

Figure 7. ***(Continued)*** **D,** splenic *Ccl19*, *Ccl21*, *Cxcl12*, and *Cxcl13* mRNA expression of *Eμ-Tcl1* mice treated with either LTβR-Ig ($n = 9$) or control Ig ($n = 9$) were analyzed by qRT-PCR. Gene expression was calculated relative to *Gapdh*. Error bars indicate mean ± SEM. *P* values were determined by the Mann–Whitney test. *, $P \leq 0.05$; **, $P \leq 0.01$; ***, $P \leq 0.001$. **E,** qRT-PCR of lymphotoxin and TNFα transcripts in sorted human (hu) B cells ($CD19^+$; $n = 4$), hu CLL B cells ($CD19^+CD5^+$; $n = 3$), and in the B-CLL cell line MEC-1 ($n = 2$). Transcript expression was normalized to *Gapdh*. Error bars indicate mean ± SEM. **F,** human MEC-1 cells (1×10^7) were i.v. transferred into *NOD/SCID/c-γ-chain*$^{-/-}$ mice. On day 3 up to day 25, mice were treated with 100 μg LTβR-Ig ($n = 3$; right) i.p. in 7-day intervals, or control mouse IgG1 (MOCP21; $n = 4$; left). Representative spleen sections were stained 28 days after transfer for $CD19^+$ MEC-1 cells (red) and $CD21^+CD35^+$ FDCs (red). Scale bars, 50 μm.

receptor CXCR5 has a dominant role in leukemia cell microanatomic localization.

Eμ-Tcl1 B cells showed a hierarchy among expressed homeostatic chemokine receptors. CXCR4 has been identified as a survival factor in CLL (39) and as an important homing receptor of neoplastic B cells to the bone marrow (40), whereas CXCR5 expression is predominantly associated with CLL positioning in SLOs (41). Although CXCL12–CXCR4 engagement accelerates human B-CLL and murine *Eμ-Tcl1* leukemia cell proliferation *in vitro*, *in vivo* this activity requires access to a CXCL12-providing niche. In our murine CLL model, CXCR5 crucially controls homing of leukemia cells into the B-cell follicles of SLOs. CXCR4 could not compensate for CXCR5 deficiency regarding their migratory functions: CXCR5-deficient leukemia cells were restricted to the MZ zone but not attracted to the B-cell follicle, and tumor cells remained absent from the dark zone of the GC, the attraction to which is CXCL12–CXCR4 governed (36).

In the absence of CXCR5, spontaneous onset of disease in *Eμ-Tcl1* mice was severely delayed. Gene expression profiling uncovered a proliferative advantage in CXCR5-expressing *Eμ-Tcl1* tumor cells, whereas no obvious differences were found in apoptosis-mediating pathways. In conjunction with a compartment-specific higher proliferation rate, this observation is in line with the view that B-CLL is not a static or accumulative disease that simply results from long-lived lymphocytes defective in apoptosis (42, 43).

Migration of normal B cells toward follicles is mediated by the CXCL13–CXCR5 signaling axis and a stromal cell network (25, 44). CXCL13, which is produced by the FDC network and MRCs, guides circulating naïve B cells in the proximity of FDCs, a prerequisite for the formation of B-cell follicles (36). Moreover, CXCR5 also plays a unique role in trafficking and homing of B-1 B cells (45). In patients with CLL, leukemia cells express high levels of functional CXCR5, and significantly higher CXCL13 serum levels were found compared with healthy controls (41).

With regard to these correlative studies in patients with CLL, we aimed to dissect the CXCR5-dependent spatial positioning of *Eμ-Tcl1* leukemia cells *in vivo*. We found that upon

Published OnlineFirst September 24, 2014; DOI: 10.1158/2159-8290.CD-14-0096

adoptive transfer, *Eμ-Tcl1* leukemia cells lodged within the splenic B-cell follicles in close proximity to FDCs. In sharp contrast, *Cxcr5*$^{-/-}$ leukemia cells accumulated in the MZ of the spleen. Bajénoff and colleagues (46) showed that T and B lymphocytes are guided by FRCs and enter the WP across MZBCs. Here, we observed that *Eμ-Tcl1* leukemia cells directly crossed the MZ sinus and reached the B-cell follicle faster than follicular B cells. Hence, leukemic cells exhibited remarkable functional similarity to MZ B-2 lymphocytes, which also shuttle directly from the MZ to the B-cell follicle (26). Gene expression profiling revealed a higher similarity of *Eμ-Tcl1* leukemia cells with B-1 B cells, as compared with MZ B cells. This result is consistent with the initial classification of these tumors (47), and would also fit with several properties of the human unmutated variant of B-CLL. Although physiologic differences between murine and human B-cell populations exist, prohibiting definitive conclusions (48), similarities are also appreciated that affect structural restriction of the BCRs, the polyreactivity toward autoantigens, expression of CD5, and the presentation as activated antigen-experienced B cells (3, 9, 49). B-1 cells can induce and associate with FDCs in mice; however, trafficking routes of these cells have not been thoroughly analyzed (50).

CXCL13–CXCR5 signaling is crucial for B-cell migration under steady-state conditions and enhances antigen encounter and BCR-triggered B-cell activation (51). A strong correlation has been proposed between antigen-stimulated BCR signaling and the clinical course of CLL (3). Involvement of a microbial-derived or autoantigen component in the heavy chain Ig repertoire selection has been suggested in many CLL cases, leading to the occurrence of stereotyped BCRs (1, 52). Alternatively, a BCR-mediated antigen-independent, cell-autonomous signaling mechanism might account for CLL signaling activity. However, this *in vitro* model does not rule out involvement of *in vivo* extrinsic antigens as additional enhancers (53).

How could *Eμ-Tcl1* leukemia B cells receive proliferation stimuli *in vivo*? Using two-photon microscopy, we found that *Eμ-Tcl1* leukemia cells showed decreased displacement rates and increased interaction times with follicular FDCs compared with leukemia cells outside this area. This could result from their cognate nature and ability to encounter antigen-laden FDCs. The preferred tumor cell localization in the FDC-rich GC light zone may also be due to the paracrine provision of growth-promoting factors (34, 35). BCR engagement, as evidenced by activated BTK, and the receipt of growth factors could act differentially during tumor ontogeny and in a complementary manner. In this view, a strong antigen dependence exists in early stages, followed by competition for natural ligand availability, then acquisition of additional oncogenic lesions, and, finally, selection for mutants that can co-opt autonomous signaling from either the BCR or their downstream effectors (54).

The differentiation of FDCs is essential for SLO organogenesis (55) and final FDC maturation crucially requires lymphoid tissue-inducer (LTi) cells and B cells expressing LTαβ (56). Consistent with previous reports that B-2 and B-1 B cells can induce the formation of mature FDC networks (50, 57), a human leukemia cell line efficiently induced FDC networks in *NOD/SCID/c-γchain*$^{-/-}$ mice. This implies that B leukemia cells themselves provide the crucial factors for FDC differentiation *in vivo*. The cross-talk between leukemic B cells and rudimentary stromal cells could be of relevance for a posttherapeutic minimal residual disease state. Irradiation of WT mice elicited an accumulation of leukemia B cells around radio-resistant FDCs and MRCs. This spatial proximity accelerated the growth rate of the tumor cells, most likely through uncompeted access to FDCs.

Notably, much of the cellular proliferation in human CLL arises in pseudofollicular proliferation centers in SLO, which are unique to CLL among all other B-cell malignancies, but they are observed in inflamed tissues of patients with systemic autoimmune disorders as well (1). Functional similarities between inflammation- and CLL-associated proliferation centers may include their capacity to initiate or maintain autoantigen stimulation, indicating that autoimmune diseases and CLL could share part of their pathogenic trait. The occurrence of FDCs in proliferation centers has been reported (58), thus supporting the view that leukemia B cell–FDC encounter is a major source of cellular proliferation.

We infer from our data that leukemia cell–associated LTαβ confers the required ligand such that FDC networks can be induced *de novo*. In this paracrine network, further FDC stimulation with cell-bound LTαβ can induce the expression of CXCL13 and other proinflammatory cytokines (59). To break this feedback loop, we treated mice with an LTβR–Ig fusion protein and found that targeting the LTβR signaling pathway profoundly retarded murine CLL growth. FDC loss and CXCL13 reduction indicated that inhibition of stroma–lymphoma cell cross-talk can translate into an ameliorated clinical course. Targeting the stromal environment in SLOs is an appealing treatment option for indolent lymphoma because these benign compartments are subject to low selective pressure for mutations and epigenetic changes (60).

We propose that our stroma induction model can mimic an early pathogenic condition in which, upon arrival of transformed clonal CLL cells in SLO, leukemia cells encounter a microenvironment that enhances their proliferation. Reciprocally, tumor cells impose stroma remodeling. Increased proliferative activity in proximity to FDC networks could enhance genetic vulnerability, resulting in mutation acquisitions that render tumor cells increasingly independent from antigenic triggering (1).

When applying an LTβR-decoy receptor, selective targeting of the stroma interface alone led to tumor growth retardation; this strategy is applicable to a minimal residual disease state in which tumor cells might be protected in LT-dependent niches. Furthermore, it may be possible to inhibit leukemia cell access to antigen-presenting cells, either through selective interference with CXCR5 activity as shown here, or by targeting the FDC function in growth factor supply. Both immunologic treatments are rational strategies to complement traditional cytotoxic therapies for the cure of leukemia and lymphoma.

METHODS

More detailed methods can be found in Supplementary Methods.

Published OnlineFirst September 24, 2014; DOI: 10.1158/2159-8290.CD-14-0096

Microarray Data

The microarray data presented in this publication have been deposited in NCBI's Gene Expression Omnibus (61) and are accessible through GEO series accession number GSE60925.

Chemotaxis Assay

Assays were performed in 5-μm-pore Transwell plates (Corning) for 4 hours at 37°C, exactly as described previously (16). CCL21, CXCL12, and CXCL13 were used at a concentration of 100 nmol/L, 25 nmol/L, and 300 nmol/L, respectively (R&D Research Diagnostics).

Patient CLL Blood Samples

Peripheral blood samples from treatment-naïve CLL patients were purified over a Ficoll gradient. Tumor cells ($CD19^+CD5^+$) were FACS-sorted and RNA was immediately extracted. The study was conducted according to the Declaration of Helsinki and in accordance with local ethical guidelines; written informed consent of all patients was obtained.

Generation of Primary Eμ-Tcl1 Leukemia Cells for Transplantation

Eμ-Tcl1 transgenic mice were monitored for signs of disease by quantification of the frequency of tumor cells in peripheral blood by flow cytometry ($CD5^+CD19^+$). Spleen-derived leukemia cell suspensions were prepared from diseased mice (>8 months old and tumor cell load >50% in the periphery) by tissue homogenization, depletion of red blood cells, and FACS sorting.

Cell Lines

Murine bone marrow stromal cells (M2-10B4; ATCC-CRL-1972) were obtained from the ATCC in July 2010. The cells were passaged two to three times over a period of 3 weeks and aliquots were frozen in liquid nitrogen. All experiments were performed with these aliquots. The human FDC line FDC/HK was obtained from Y.S. Choi (Ochner Clinic foundation, New Orleans, LA) in 2011 and cultured as described above. No further authentication was done for both cell lines.

In Vivo *Blockade of the LTβ-Receptor Signaling Pathway*

Blocking LtβR–Ig [100 μg; murine receptor fused to mouse mAb IgG1; Biogen Idec or generated as described previously (62)] or isotype control antibody (MOPC 21) were injected repeatedly i.p. into tumor challenged and *Eμ-Tcl1* transgenic mice, respectively.

Statistical Analysis

Results are expressed as arithmetic means ± SEM if not otherwise indicated. Values of $P \leq 0.05$ were considered statistically significant, as determined by the unpaired Mann–Whitney test, the two-tailed unpaired Student *t* test, or the Wilcoxon signed rank test where appropriate.

Disclosure of Potential Conflicts of Interest

No potential conflicts of interest were disclosed.

Authors' Contributions

Conception and design: A.E. Hauser, G. Lenz, A. Rehm, U.E. Höpken
Development of methodology: K. Heinig, V. Stache, A.E. Hauser, R. Brink, U.E. Höpken
Acquisition of data (provided animals, acquired and managed patients, provided facilities, etc.): K. Heinig, M. Gätjen, I. Anagnostopoulos, K. Gerlach, R.A. Niesner, Z. Cseresnyes, A.E. Hauser, T. Hehlgans, J. Westermann, A. Rehm
Analysis and interpretation of data (e.g., statistical analysis, biostatistics, computational analysis): M. Gätjen, M. Grau, V. Stache, I. Anagnostopoulos, R.A. Niesner, Z. Cseresnyes, A.E. Hauser, P. Lenz, J. Westermann, G. Lenz, A. Rehm, U.E. Höpken
Writing, review, and/or revision of the manuscript: K. Heinig, M. Grau, R.A. Niesner, A.E. Hauser, T. Hehlgans, J. Westermann, B. Dörken, M. Lipp, G. Lenz, A. Rehm, U.E. Höpken
Administrative, technical, or material support (i.e., reporting or organizing data, constructing databases): A.E. Hauser, R. Brink, A. Rehm
Study supervision: B. Dörken, M. Lipp, A. Rehm, U.E. Höpken

Acknowledgments

The authors thank Carlo Croce (Columbus University, Columbus, OH) and Jeffrey L. Browning (Biogen Idec, Cambridge, MA) for providing essential reagents and Heike Schwede and Kerstin Krüger for excellent technical assistance.

Grant Support

This work was funded by grants from the Deutsche Krebshilfe (grant number 107749), German Research Foundation (DFG), and the Berliner Krebsgesellschaft to U.E. Höpken and A. Rehm; grants from the DFG, the Deutsche Krebshilfe, and the Else Kröner-Fresenius-Stiftung to G. Lenz; the DFG-funded project "JIMI-a network for intravital microscopy" to R.A. Niesner, Z. Cseresnyes, and A.E. Hauser; and by a Doctoral Scholarship from the Philipps-Universität Marburg to M. Grau.

The costs of publication of this article were defrayed in part by the payment of page charges. This article must therefore be hereby marked *advertisement* in accordance with 18 U.S.C. Section 1734 solely to indicate this fact.

Received January 28, 2014; revised September 11, 2014; accepted September 12, 2014; published OnlineFirst September 24, 2014.

REFERENCES

1. Caligaris-Cappio F. Inflammation, the microenvironment and chronic lymphocytic leukemia. Haematologica 2011;96:353–5.
2. Munk Pedersen I, Reed J. Microenvironmental interactions and survival of CLL B-cells. Leuk Lymphoma 2004;45:2365–72.
3. Zenz T, Mertens D, Kuppers R, Dohner H, Stilgenbauer S. From pathogenesis to treatment of chronic lymphocytic leukaemia. Nat Rev Cancer 2010;10:37–50.
4. Ishibe N, Sgambati MT, Fontaine L, Goldin LR, Jain N, Weissman N, et al. Clinical characteristics of familial B-CLL in the National Cancer Institute Familial Registry. Leuk Lymphoma 2001;42:99–108.
5. Küppers R. Mechanisms of B-cell lymphoma pathogenesis. Nat Rev Cancer 2005;5:251–62.
6. Seifert M, Sellmann L, Bloehdorn J, Wein F, Stilgenbauer S, Durig J, et al. Cellular origin and pathophysiology of chronic lymphocytic leukemia. J Exp Med 2012;209:2183–98.
7. Klein U, Tu Y, Stolovitzky GA, Mattioli M, Cattoretti G, Husson H, et al. Gene expression profiling of B cell chronic lymphocytic leukemia reveals a homogeneous phenotype related to memory B cells. J Exp Med 2001;194:1625–38.
8. Rosenwald A, Alizadeh AA, Widhopf G, Simon R, Davis RE, Yu X, et al. Relation of gene expression phenotype to immunoglobulin mutation genotype in B cell chronic lymphocytic leukemia. J Exp Med 2001;194:1639–47.
9. Chiorazzi N, Ferrarini M. Cellular origin(s) of chronic lymphocytic leukemia: cautionary notes and additional considerations and possibilities. Blood 2011;117:1781–91.
10. Kikushige Y, Ishikawa F, Miyamoto T, Shima T, Urata S, Yoshimoto G, et al. Self-renewing hematopoietic stem cell is the primary target in pathogenesis of human chronic lymphocytic leukemia. Cancer Cell 2011;20:246–59.

Published OnlineFirst September 24, 2014; DOI: 10.1158/2159-8290.CD-14-0096

11. Dohner H, Stilgenbauer S, Benner A, Leupolt E, Krober A, Bullinger L, et al. Genomic aberrations and survival in chronic lymphocytic leukemia. N Engl J Med 2000;343:1910–6.
12. Herling M, Patel KA, Weit N, Lilienthal N, Hallek M, Keating MJ, et al. High TCL1 levels are a marker of B-cell receptor pathway responsiveness and adverse outcome in chronic lymphocytic leukemia. Blood 2009;114:4675–86.
13. Bichi R, Shinton SA, Martin ES, Koval A, Calin GA, Cesari R, et al. Human chronic lymphocytic leukemia modeled in mouse by targeted TCL1 expression. Proc Natl Acad Sci U S A 2002;99:6955–60.
14. Pals ST, de Gorter DJ, Spaargaren M. Lymphoma dissemination: the other face of lymphocyte homing. Blood 2007;110:3102–11.
15. Burger JA, Kipps TJ. Chemokine receptors and stromal cells in the homing and homeostasis of chronic lymphocytic leukemia B cells. Leuk Lymphoma 2002;43:461–6.
16. Höpken UE, Foss HD, Meyer D, Hinz M, Leder K, Stein H, et al. Up-regulation of the chemokine receptor CCR7 in classical but not in lymphocyte-predominant Hodgkin disease correlates with distinct dissemination of neoplastic cells in lymphoid organs. Blood 2002;99:1109–16.
17. Höpken UE, Rehm A. Homeostatic chemokines guide lymphoma cells to tumor growth-promoting niches within secondary lymphoid organs. J Mol Med 2012;90:1237–45.
18. Gine E, Martinez A, Villamor N, Lopez-Guillermo A, Camos M, Martinez D, et al. Expanded and highly active proliferation centers identify a histological subtype of chronic lymphocytic leukemia ("accelerated" chronic lymphocytic leukemia) with aggressive clinical behavior. Haematologica 2010;95:1526–33.
19. Liberzon A, Subramanian A, Pinchback R, Thorvaldsdottir H, Tamayo P, Mesirov JP. Molecular signatures database (MSigDB) 3.0. Bioinformatics 2011;27:1739–40.
20. Kanehisa M, Goto S, Sato Y, Furumichi M, Tanabe M. KEGG for integration and interpretation of large-scale molecular data sets. Nucleic Acids Res 2012;40(Database issue):D109–14.
21. Yan XJ, Albesiano E, Zanesi N, Yancopoulos S, Sawyer A, Romano E, et al. B cell receptors in TCL1 transgenic mice resemble those of aggressive, treatment-resistant human chronic lymphocytic leukemia. Proc Natl Acad Sci U S A 2006;103:11713–8.
22. Rehm A, Mensen A, Schradi K, Gerlach K, Wittstock S, Winter S, et al. Cooperative function of CCR7 and lymphotoxin in the formation of a lymphoma-permissive niche within murine secondary lymphoid organs. Blood 2011;118:1020–33.
23. Seke Etet PF, Vecchio L, Nwabo Kamdje AH. Interactions between bone marrow stromal microenvironment and B-chronic lymphocytic leukemia cells: any role for Notch, Wnt and Hh signaling pathways? Cell Signal 2012;24:1433–43.
24. Komori T. Regulation of bone development and maintenance by Runx2. Front Biosci 2008;13:898–903.
25. Bajenoff M, Egen JG, Koo LY, Laugier JP, Brau F, Glaichenhaus N, et al. Stromal cell networks regulate lymphocyte entry, migration, and territoriality in lymph nodes. Immunity 2006;25:989–1001.
26. Cinamon G, Zachariah MA, Lam OM, Foss FW Jr, Cyster JG. Follicular shuttling of marginal zone B cells facilitates antigen transport. Nat Immunol 2008;9:54–62.
27. Gatto D, Brink R. B cell localization: regulation by EBI2 and its oxysterol ligand. Trends Immunol 2013;34:336–41.
28. Chen L, Widhopf G, Huynh L, Rassenti L, Rai KR, Weiss A, et al. Expression of ZAP-70 is associated with increased B-cell receptor signaling in chronic lymphocytic leukemia. Blood 2002;100:4609–14.
29. Herman SE, Gordon AL, Hertlein E, Ramanunni A, Zhang X, Jaglowski S, et al. Bruton tyrosine kinase represents a promising therapeutic target for treatment of chronic lymphocytic leukemia and is effectively targeted by PCI-32765. Blood 2011;117:6287–96.
30. Woyach JA, Bojnik E, Ruppert AS, Stefanovski MR, Goettl VM, Smucker KA, et al. Bruton's tyrosine kinase (BTK) function is important to the development and expansion of chronic lymphocytic leukemia (CLL). Blood 2014;123:1207–13.
31. Woyach JA, Furman RR, Liu TM, Ozer HG, Zapatka M, Ruppert AS, et al. Resistance mechanisms for the Bruton's tyrosine kinase inhibitor ibrutinib. N Engl J Med 2014;370:2286–94.
32. Gobessi S, Laurenti L, Longo PG, Sica S, Leone G, Efremov DG. ZAP-70 enhances B-cell-receptor signaling despite absent or inefficient tyrosine kinase activation in chronic lymphocytic leukemia and lymphoma B cells. Blood 2007;109:2032–9.
33. Kim HS, Zhang X, Klyushnenkova E, Choi YS. Stimulation of germinal center B lymphocyte proliferation by an FDC-like cell line, HK. J Immunol 1995;155:1101–9.
34. Mourcin F, Pangault C, Amin-Ali R, Ame-Thomas P, Tarte K. Stromal cell contribution to human follicular lymphoma pathogenesis. Front Immunol 2012;3:280.
35. El Shikh ME, Pitzalis C. Follicular dendritic cells in health and disease. Front Immunol 20123:292.
36. Allen CD, Ansel KM, Low C, Lesley R, Tamamura H, Fujii N, et al. Germinal center dark and light zone organization is mediated by CXCR4 and CXCR5. Nat Immunol 2004;5:943–52.
37. Green JA, Suzuki K, Cho B, Willison LD, Palmer D, Allen CD, et al. The sphingosine 1-phosphate receptor S1P(2) maintains the homeostasis of germinal center B cells and promotes niche confinement. Nat Immunol 2011;12:672–80.
38. Roozendaal R, Mebius RE. Stromal cell–immune cell interactions. Annu Rev Immunol 2011;29:23–43.
39. Burger JA. Chemokines and chemokine receptors in chronic lymphocytic leukemia (CLL): from understanding the basics towards therapeutic targeting. Semin Cancer Biol 2010;20:424–30.
40. Burger JA, Burger M, Kipps TJ. Chronic lymphocytic leukemia B cells express functional CXCR4 chemokine receptors that mediate spontaneous migration beneath bone marrow stromal cells. Blood 1999;94:3658–67.
41. Burkle A, Niedermeier M, Schmitt-Graff A, Wierda WG, Keating MJ, Burger JA. Overexpression of the CXCR5 chemokine receptor, and its ligand, CXCL13 in B-cell chronic lymphocytic leukemia. Blood 2007;110:3316–25.
42. Messmer BT, Messmer D, Allen SL, Kolitz JE, Kudalkar P, Cesar D, et al. *In vivo* measurements document the dynamic cellular kinetics of chronic lymphocytic leukemia B cells. J Clin Invest 2005;115:755–64.
43. Herishanu Y, Perez-Galan P, Liu D, Biancotto A, Pittaluga S, Vire B, et al. The lymph node microenvironment promotes B-cell receptor signaling, NF-kappaB activation, and tumor proliferation in chronic lymphocytic leukemia. Blood 2011;117:563–74.
44. Forster R, Mattis AE, Kremmer E, Wolf E, Brem G, Lipp M. A putative chemokine receptor, BLR1, directs B cell migration to defined lymphoid organs and specific anatomic compartments of the spleen. Cell 1996;87:1037–47.
45. Höpken UE, Achtman AH, Kruger K, Lipp M. Distinct and overlapping roles of CXCR5 and CCR7 in B-1 cell homing and early immunity against bacterial pathogens. J Leukoc Biol 2004;76:709–18.
46. Bajenoff M, Glaichenhaus N, Germain RN. Fibroblastic reticular cells guide T lymphocyte entry into and migration within the splenic T cell zone. J Immunol 2008;181:3947–54.
47. Pekarsky Y, Calin GA, Aqeilan R. Chronic lymphocytic leukemia: molecular genetics and animal models. Curr Top Microbiol Immunol 2005;294:51–70.
48. Pillai S, Cariappa A. The follicular versus marginal zone B lymphocyte cell fate decision. Nat Rev Immunol 2009;9:767–77.
49. Martin F, Kearney JF. B1 cells: similarities and differences with other B cell subsets. Curr Opin Immunol 2001;13:195–201.
50. Wen L, Shinton SA, Hardy RR, Hayakawa K. Association of B-1 B cells with follicular dendritic cells in spleen. J Immunol 2005;174:6918–26.
51. Saez de Guinoa J, Barrio L, Mellado M, Carrasco YR. CXCL13/CXCR5 signaling enhances BCR-triggered B-cell activation by shaping cell dynamics. Blood 2011;118:1560–9.
52. Fais F, Ghiotto F, Hashimoto S, Sellars B, Valetto A, Allen SL, et al. Chronic lymphocytic leukemia B cells express restricted

Published OnlineFirst September 24, 2014; DOI: 10.1158/2159-8290.CD-14-0096

sets of mutated and unmutated antigen receptors. J Clin Invest 1998;102:1515–25.
53. Duhren-von Minden M, Ubelhart R, Schneider D, Wossning T, Bach MP, Buchner M, et al. Chronic lymphocytic leukaemia is driven by antigen-independent cell-autonomous signalling. Nature 2012;489:309–12.
54. Greaves M. Clonal expansion in B-CLL: fungal drivers or self-service? J Exp Med 2013;210:1–3.
55. Fu YX, Huang G, Wang Y, Chaplin DD. B lymphocytes induce the formation of follicular dendritic cell clusters in a lymphotoxin alpha-dependent fashion. J Exp Med 1998;187:1009–18.
56. Tumanov A, Kuprash D, Lagarkova M, Grivennikov S, Abe K, Shakhov A, et al. Distinct role of surface lymphotoxin expressed by B cells in the organization of secondary lymphoid tissues. Immunity 2002;17:239–50.
57. Gonzalez M, Mackay F, Browning JL, Kosco-Vilbois MH, Noelle RJ. The sequential role of lymphotoxin and B cells in the development of splenic follicles. J Exp Med 1998;187:997–1007.
58. Schmid C, Isaacson PG. Proliferation centres in B-cell malignant lymphoma, lymphocytic (B-CLL): an immunophenotypic study. Histopathology 1994;24:445–51.
59. Ansel KM, Ngo VN, Hyman PL, Luther SA, Forster R, Sedgwick JD, et al. A chemokine-driven positive feedback loop organizes lymphoid follicles. Nature 2000;406:309–14.
60. Acharyya S, Oskarsson T, Vanharanta S, Malladi S, Kim J, Morris PG, et al. A CXCL1 paracrine network links cancer chemoresistance and metastasis. Cell 2012;150:165–78.
61. Edgar R, Domrachev M, Lash AE. Gene Expression Omnibus: NCBI gene expression and hybridization array data repository. Nucleic Acids Res 2002;30:207–10.
62. Stopfer P, Obermeier F, Dunger N, Falk W, Farkas S, Janotta M, et al. Blocking lymphotoxin-beta receptor activation diminishes inflammation via reduced mucosal addressin cell adhesion molecule-1 (MAdCAM-1) expression and leucocyte margination in chronic DSS-induced colitis. Clin Exp Immunol 2004;136:21–9.

Published OnlineFirst September 24, 2014; DOI: 10.1158/2159-8290.CD-14-0096

CANCER DISCOVERY

Access to Follicular Dendritic Cells Is a Pivotal Step in Murine Chronic Lymphocytic Leukemia B-cell Activation and Proliferation

Kristina Heinig, Marcel Gätjen, Michael Grau, et al.

Cancer Discovery 2014;4:1448-1465. Published OnlineFirst September 24, 2014.